TIME SERIES ANALYSIS OF POWER REQUIREMENTS FOR TILLAGE TOOLS

by

NAOMI KAY REGIER

B.S., Kansas State University, 1983

A MASTER'S THESIS

submitted in partial fulfillment of the

requirements for the degree

MASTER OF SCIENCE

Department of Agricultural Engineering

KANSAS STATE UNIVERSITY
Manhattan, Kansas

1986

Approved by:

Mark D. Schrock
Major Professor

Time Series Analysis of Power Requirements for Tillage Tools
(Naomi K. Regier, M. S. 1986)

TABLE OF CONTENTS

ACKNOWLEDGEMENTS

The author would like to express her thanks to Dr. Mark Schrock for his time and encouragement in support of this project. Thanks are also expressed to the other members of her committee for their time spent reviewing this thesis.

Thanks are also due to Dr. Winston Yang, of the KSU Department of Statistics, for his time spent in helpful discussions of the pros and cons of different analysis techniques.

Thanks also go to Richard H. Jones, of the Department of Preventive Medicine and Biometrics, School of Medicine at the University of Colorado Health Sciences Center, for making available helpful reference materials along with a computer program for ARMA analysis of data with missing values.

Not to be forgotten are my fellow graduate students, as well as others who work on computers, for their encouragement and willingness to share computer time. The computer system managers also deserve mention for their patience with the programs used in this study.

Last, but certainly not least, a deep appreciation is expressed to Wilbert and Lydia Regier, parents of the author, for their loving support and prayers throughout her education.

INTRODUCTION

In the last twenty years, the operating environment of farm tractors has changed drastically in size and ergonomics. The environment has become quite comfortable, particularly on the larger tractors. Often, operators tend to use their more comfortable tractors to perform even the light-duty tasks which do not utilize the full power of the big machines. When a large tractor is operating under a light load, fuel can potentially be saved. Most operators tend to operate the engine at a higher engine RPM than necessary; if they would gear up the transmission and lower the RPM, they could move to a more fuel-efficient location in the engine load map while still producing the same power output.

To this end, extension personnel at Kansas State University have encouraged an adjustment in operating practices, called gear up and throttle back. A concern expressed by some operators about this change in driving habits was that they might, inadvertently, throttle the engine down to a range that could damage it under sustained low speed operation. To avoid such an occurrence, a gear selection aid was developed (Blumanhourst, 1984), (Blumanhourst, et al. 1984). The device monitored the power being used and displayed a new engine speed, gear ratio, and fuel savings if more than .5 gal/hr of fuel could be saved by switching from the present to the new setting. The device was generally successful at saving fuel, although the amount saved depended on the operating habits of the person and the nature of the load. The .5 gal/hr figure was used as the minimum to prevent the algorithm from constantly recommending minor changes in gears and engine speeds for insignificant fuel savings. The use of the threshold implies that potential fuel savings still exist even if the device recommendations are followed

faithfully. Blumanhourst (1984, Fig. 6) shows that more fuel can be saved by increasing shift frequency. However, in the range of 20-30 shifts/hr, the fuel savings is small compared to the inconvenience of shifting often.

Histograms obtained by Blumanhourst showed variations both within a field operation and between field operations. For some operations where the load varies only slightly, many of the load changes may be below the level that would translate to significant fuel savings if the gears were shifted. For the more abrupt load changes common to primary tillage tools, fuel savings could also be difficult to realize due to the impossibility of shifting fast enough to maximize the savings.

The present project seeks to capture the potential fuel savings by using a continuously-variable transmission to more closely approximate the point of maximum fuel efficiency. The laboratory setup consists of a Caterpillar 3304 engine coupled to a Vadetec continuously-variable transmission (CVT) in series with a Funk power-shift transmission and planetary gearbox with a Midwest eddy-current dynamometer loading the system. The entire system is under computer control so that the engine will remain in the most fuel-efficient area of the engine map.

To test the control algorithm for stability and actual fuel savings, a "typical" pattern of loading due to tillage patterns will be needed. Data files from the gear selection aid project were used to provide the test patterns. The many hours of collected data were to be condensed and represented by a short 10-15 minute sample. Methods such as selecting a short piece of data, using the increment from the last reading, or deviation about a local mean were considered. Finally, it was decided to represent the pattern using

statistical methods such as spectral density or autoregressive-moving average processes. Thus, a short cycle could be characteristic of the hours of data collected in the field.

OBJECTIVE

The objective of this study was to represent various tillage implements by characteristic power series obtained from data of previous field trials.

LITERATURE REVIEW

Standards and Soil Models

For guidelines on how to derive a typical test cycle simulating field tillage on a dynamometer, one potential source is the tractor test standards published by the engineering societies. In the United States, the American Society of Agricultural Engineers (ASAE S209.5) and the Society of Automotive Engineers (SAE J708 JUN80) use the same standard to test the claims of the manufacturer. These tests subject the tractor to drawbar, PTO, and fuel consumption tests. The testing is done on a hard surface at a constant speed for consistency and convenience. The International Organization for Standardization also lists standards (ISO 789/1) which are similar to the ASAE and SAE standards for testing tractors.

Relationships betwleen the variables which affect a tractor's performance on a hard surface may relate test track data to actual working conditions. Information, including graphs, on variables such as the wheel loading factor, tractor size and configuration, and tractive performance on a concrete surface is given by Leviticus and Reyes (1985). In addition, ASAE standard D230.3

gives guidelines to predict field performance from test data and estimate the expected draft/unit cross section for various tools.

The above test procedures all deal with a constant level of power. These methods work satisfactorily for checking durability and estimating average fuel consumption. However, the load histograms obtained by Blumanhourst (1984) show that the load does not remain constant, but varies as the tractor progresses through the field.

The change in draft force while pulling tools through the field perhaps could be calculated by using soil models to give a test cycle which imitates the loading on a tool. However, these models are still in an elementary stage of development. Grisso and Perumpral (1985) evaluate different soil models, all of which use the basic wedge in front of the tool to calculate the draft force and make other simplifying assumptions such as uniform soil which would tend to make the load constant.

Industry Simulations from Data

Industry and government use road simulations to test a variety of vehicles without the expense of field testing. The Environmental Protection Agency prescribes a sequence of automobile speeds to check exhaust gas emissions (SAE J1094a) using a dynamometer. On actual roads, the road profiles can be examined (see Chaka (1978) for a description of an electronic road profiler) to verify that no changes in input have occurred to vehicles on durability tests. Chaka also says that the road profiles are useful in duplicating public road profiles on special test roads.

Histograms have been used to simulate the conditions of a tractor in the field (Whelpley, 1973). Field data of axle torque was collected and analyzed to produce frequency of occurrence histograms of various field operations. A histogram using 20 load increments was constructed for each unique field operation. The individual histograms were then combined on a time-weighted basis to produce master histograms for a specific operation (i. e. third-gear operation using heavy draft implements). These histograms were then used to make master histograms for the engine and the drive train. The field data was combined based on percent of time spent at heavy, medium, and light draft loads to make a final histogram consisting of ten blocks. For the engine histogram, data from all gears was used in proportion to the amount of actual field usage. For the power train, the histogram consisted only of data for a specific gear ratio. The load levels for the dynamometer were then selected through a randomized block sequence. The final histogram could also be represented in continuous form by the amplitude probability distribution (Bekker, 1969), which uses a single curve to display the load levels. As an alternative to the histograms, Whelpley also considered using a mean torque signal combined with a random signal to simulate the deviation of the load history.

Cryer and Nawrocki (1976) used spectral density to determine the inputs for a road simulator. Four basic steps were used in this approach. First, the vehicle was driven on a road of interest while instruments recorded the vertical acceleration on each wheel spindle. Second, the vehicle was placed on appropriate actuators and the dynamic characteristics which relate the spindle response to the actuator inputs were measured. Third, using the desired response obtained from the test road, the effective road inputs were

derived by using the dynamic characteristics of the test stand. Fourth, the response to the derived inputs was determined and compared to the desired response. The actuator inputs were then varied iteratively until the power spectral density plots for the simulated road profile matched that obtained for the actual surface. Cryer and Nawrocki (p. 2) report that "the PSD description of road profiles is gaining acceptance, since it is an accurate description of the road" and that it has been proposed to the ISO as a standard description of road roughness.

Time Series Models

Evenly-Spaced Methods

Several methods of analyzing time series are widely encountered in the literature. Two closely-linked methods are autocovariance, commonly displayed as autocovariance versus lag, and spectral analysis which maps the relative covariance, known as power spectral density, versus frequency. The autocovariance shows patterns, if any, as the time variable changes while power spectral density shows whether the spectrum has peaks of variance in narrow frequency ranges, as would be the case with a cosine curve, or whether the relative covariance changes gradually over a wide frequency range. The classic text on spectral density analysis, and with it autocovariance, was written by Blackman and Tukey (1958). The theory is now covered in many books that deal with time series analysis. The basic theory is outlined in Appendix A along with a procedure used by Walls et al. (1954) and Wendenborn (1966) to generate PSD plots for discrete data.

Another type of time series analysis consists of the AutoRegressive and Moving Average, ARMA(p,q), models which Box and Jenkins (1976) deal with

extensively. These models consist of three parts, the autoregressive, the moving average, and the random plant noise. The autoregressive part makes the present value dependent on p past values, each multiplied by a distinct coefficient which reflects the degree of dependency. The moving average part makes the present value dependent on q past random noises. The random noise term, present in all models even if q is zero, is added to reflect the assumption that the next value is not determined absolutely, but will fall within a certain range, assumed to be gaussian in distribution.

Irregularly-Spaced Methods

The theory for time series analysis methods like power spectral density or the ARMA models has been well-developed for continuous or evenly-spaced data (see Otnes and Enochson (1972) or Box and Jenkins (1976)). Only recently have methods been suggested for dealing with irregularly-spaced data. Various methods for analyzing irregular time series are given by Parzen (1984).

Irregular spacing can be dealt with by weighting the individual elements. Masry (1984) uses a mean value of sampling rate which is a constant in his spectral density calculations. Marquardt and Acuff (1984) weight the i,jth element's contribution to the spectral density by the proportion of time represented in a square containing that element. An attempt was made to analyze the available data using this method (see "Methodology"). The Direct Quadratic Spectrum Estimation (DQSE) method developed by Marquardt and Acuff is summarized in Appendix B.

Harvey and Pierse (1984) describe an ARMA method that is useful when the data was taken at long intervals initially and then later taken at closer intervals, as would be the case with stock prices which were recorded yearly

at first, and later changed to monthly index. Their technique reverses the series so to obtain the initial covariance matrix. The state space approach is then used to evaluate the parameters with an optimization program which uses numerical derivatives to fit the parameters. They also show an approach for evaluating an AutoRegressive Integrated Moving Average (ARIMA) method for use with differencing, the change between the data points instead of the actual points, and seasonal differencing.

Jones (1980, 1985a) details an ARMA method which is useful for cases of evenly-spaced data with missing values. The method uses the state space approach on a given data set. The initial covariance matrix is calculated recursively from the expected data values, which can be expressed in terms of the coefficients of past values and random noise. The scheme of model fitting begins with initial estimates of the parameters and then uses a nonlinear optimization program to vary the parameter values until the minimum value of -2 ln(likelihood) is reached. This method is described further under the section entitled "Theory of the ARMA Process". Jones also considers the ARMA method for the case of data with irregular spacing (Jones, 1985b).

In the ARMA(p,q) model, which bases the present value upon p past values and q past random plant noises, the accuracy of the estimate of the p and q coefficients used with the past values can be judged by any of several guidelines (see Jones (1985a) for a summary). The least squares approach selects the value that minimizes the sum of squares of the residual. The Yule-Walker equations choose the parameters which best predict the present covariances from the past covariances. The maximum entropy approach is similar to least squares, except that a backwards autoregression is considered. Forward and backward autoregressions converge to the same value. The term in the

numerator for the parameters is the same for both directions, but the denominator differs by a term. Burg's maximum entropy estimate uses an average of the two denominators from forward and backward autoregression as the denominator.

Yet another way of estimating the best fit, under the assumption that the noises are normally distributed, is the likelihood function which depends upon a combination of the innovation; that is, the difference between the actual and predicted values, and the variance of the innovation. The likelihood function is often simplified to ln(likelihood). The relative value of likelihood for a data set is considered rather than the absolute since the value differs according to the type and length of the data sample. Akaike (1974) makes another modification to the likelihood function by adding a penalty for increasing the order of the autoregression. Akaike's Information Criterion (AIC) is meant to be an estimate of 2N times the average information for distinguishing between the assumed and true model, where N is the number of data points. The first part, consisting of -2 ln(likelihood), is the penalty for the badness of fit between the modeled value and the actual value in the data. The second part, the addition of twice the number of parameters, is the penalty for increased unreliability caused by using an increasing number of variables to describe the system. In the concept of the AIC number, the best model is the one with the lowest AIC value. Models with an AIC value close to the lowest can also be considered, with a lower order model being preferable to a more complicated model.

ORIGINAL DATA COLLECTION

The raw data collected in the original gear selection aid project consisted of time, engine and transmission hertz signal counts, and position of the injector pump rack. The transmission ratio and ground speed were thus easily obtained. The power and fuel flow were obtained by regression equations from rack position and rpm. The specific fuel consumption was then easily calculated. The above values were recorded; the variables considered in the present analysis are time, velocity, and power.

The instrumentation sampled the data points at a rate of 1 sample/sec. At the time of the experiment, the interest was in the overall patterns so a long time-length sample was desired to accurately estimate the load histogram. Tape was chosen as a storage media, so in order to work within the storage space of the microcomputer and minimize the tape-writing time, the sampled values were recorded in the cycle described below and shown in Fig. 1.

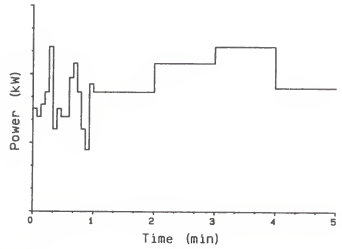

Figure 1. Data Cycle

1. Readings were taken each second.

2. For the first minute of the 5-minute cycle, the data was stored as 15 4-second averages. The data treated in this way will be referred to as fine data.

3. The subsequent 4 minutes of readings were stored as 4 1-minute averages. The data treated in this manner will be referred to as coarse data.

The short-term (4-sec) averages showed the faster variations while the 60-sec averages showed the long-terms variations in loading patterns. The result of the data was used to plot histograms of power-usage variation (Blumanhourst, 1984). The data files contained several segments of data since the original project disregarded values when the gears were shifted or the tractor was traveling from one location to another. The longest "continuous" data segment was used to represent each file. A FORTRAN program checked the fine and coarse values for the beginning and end of the segment. The end occurred if values were missing when the total accumulated time was less than or equal to 5 minutes or when the count was above 30 minutes and the time skipped was greater than or equal to 10 minutes. The total sample length varied by location and ranged from 30 minutes to over 4 hours.

MATERIALS

The materials used in the current analysis consisted of the data files, collected as described above, computers to analyze the data, and programs to control the data processing. A DEC PDP 11/34 was used to run the first two methods of analysis using a spectral density approach. A Harris 800 was used to run Jones' exact likelihood method due to the speed of the Harris and the amount of iteration necessary in the program. The three methods considered for analysis are described below.

METHODOLOGY

Analysis of the series was attempted using three different methods. The first two attempts were based on the idea that any pattern can be represented as a collection of sine and cosine waves. The third method of analysis assumed that the present value is dependent on the past values as well as on random noises.

Regularly-Spaced Spectral Density

The first analysis attempt used Blackman and Tukey's power spectral density which deals with regularly-spaced data with no missing values (Walls, et al,1954) and (Wendenborn, 1966). Since the available data was evenly spaced with missing values in the coarse segments, it was forced into evenly-spaced intervals by recombining the data. The basic interval used was the 4-second interval. The mean of each minute of data was determined. For the first minute of the data-taking cycle, this was the mean of 15 points. For the remaining four minutes, this was simply the recorded value, since this was already the average over 60 seconds. The data was then recombined starting with the first minute of fine data. The deviations from the one-minute mean of the fine data were determined. The data was then reorganized by combining the deviations of the fine data from minutes 1,6,11,16,21,... about the means of minutes 1,2,3,4,5,.... This recombined data was then analyzed by the autocorrelation-fourier transform method described in Appendix A. Since there was little, if any, statistical support for the above recombination of data. the search was continued for methods that were suitable for the data spacing pattern.

Direct Quadratic Spectrum Estimation

Marquardt and Acuff's Direct Quadratric Spectrum Estimation (DQSE) method was used in the second approach (Marquardt and Acuff, 1984). This method calculates the spectrum by giving a weighting factor, which is dependent on the time since the last sample, to each correlation value. The samples are assumed to be point samples taken at irregular intervals. Since the algorithm had the capability of dealing with irregular spacing, the samples were analyzed on a distance basis, as determined from the average speed at each data sampling, instead of on a time basis. The data in the present case is not a point sample, but rather an average. The fine samples are close enough to be regarded as point samples, and indeed, the apparent amplitudes in averaged data and the point samples can be related by regression. The minute averages are too different from the 4-sec averages to be regarded as point values and so they are left out of the spectral density analysis by the DQSE method. The Marquardt-Acuff algorithm is given in Appendix B.

The most obvious result of the weighting by time intervals is that the beginning and end values of the minute of fine data, within the sample, are given a much larger weight than the other values in the minute. Consequently, known curves in the form $A \cos(2*\pi x/T)$ where A is the amplitude, T is the period, and t is the time were also analyzed by this method. The known curve was treated in the same manner as the original data. Values were calculated at 1 second intervals. For the first minute, 15 values were recorded, each consisting of averages over 4 seconds. The next four minutes were not recorded, as they are not representative of the same area as the 4-second value. The cycle was repeated until a suitable length was obtained. On the spectral density plot of a known curve, an abrupt peak occurs at the expected

frequency. On either side are prominent side lobes, their presence due to leakage and their height to the effect of irregular spacing. These lobes make interpretations of the resulting spectrum inexact. In order to obtain a sharp window which focuses only on the frequency under consideration, as recommended by Marquardt and Acuff, the lag was long enough to stretch over several 5-minute cycles.

An attempt was made to relate the main peak in the spectral density plot of a known curve to the original amplitude by regression equations. The factors affecting the height were mainly the amplitude, A, of the original curve, and to a lesser degree, the length of the data sample and the period, T, of the wave (due to the averaging). The regression equations showed a poor degree of correlation with a changing rate of variance so this approach was reexamined by limiting the weight assigned to each data value. With the original Marquardt-Acuff approach, the weight was assigned to the minimum of the length of the Nyquist wavelength and the halfway distance between the data-taking intervals. This resulted in the starting and ending points of the data being given much greater weight than any other values. Limiting the weight that could be assigned to each point by setting the maximum possible distance to 10 m, which was approximately the distance represented in each 4-second interval in the data samples, eliminated most of the sharp peaks and gave a spectrum that was quite flat. Since the influence of the beginning and end values of the fine data samples could be unpredictable, yet another method was sought.

Autoregressive-Moving Average Approach

The third and last means of analyzing the data is the autoregressive moving average (ARMA) approach. Jones (1980,1985a) shows an adaptation of the ARMA process to deal with missing data. A way to recursively estimate the parameters is (Jones,1980) by changing to the state space form as derived by Akaike (1974). The fit of the model is evaluated by minimizing the -2 ln(likelihood) function. The model calculates likelihood where the data exists and ignores portions of nonexistent values. Thus, the value is exact for the given data. See the section "Theory of the ARMA Process" for more detail.

The model fitting was done by using a set of subroutines written by Jones (1978). The main program was based on one supplied by Jones and modified to read in the data, figure the average and standard deviation, and subtract the average from the data values to yield numbers distributed about zero. As in the DQSE approach, only the fine values were used; the coarse were neglected. The program checked 40 models in the form ARMA(p,q), with varying integers as p and q values. The AR value p ranges from 0 to 6 and the MA value q from 0 to 5. The sum of p and q is $\leq$ 10, due to program limitations, so the highest order model is ARMA(6,4). When the order of p or q is increased, the value of the transformed new variable is set to zero and the parameter values from the previous model are used to initialize the present model. If a problem is encountered in finding the minimum -2 ln(likelihood) in the previous model, such as exceeding the iteration limit, the array of transformed parameters is reset to zero for the next model. The subroutines calculate the -2 ln(likelihood) function and then feed the parameters into a non-linear optimization system which varies the transformed parameter values until the -2

ln(likelihood) is minimized. After the optimization routine has completed its work, the main program prints the output and begins the next model. After all 40 models have been evaluated, the valid solutions are sorted into ascending order of AIC (Akaike's Information Criteria is the sum of -2 ln(likelihood) plus twice the number of parameters used in the model.) and the orders of p, q, their coefficients, estimated error variance, and AIC are printed.

The optimization program used in this experiment was developed at the National Center for Atmospheric Research in Boulder, Colorado. It finds the local minimum of a twice continuously-differentiable real-valued function f from a given starting point x_0. The input for this subroutine consists of the dimension, n, of the problem, a subroutine to evaluate the function. in this case the -2 ln(likelihood) function, and an estimate x_0 of the minimum of the function. When the program is finished, the values returned are an approximation to the local minimum, the value of the gradient, and a flag to designate the reason for stopping. Termination may not necessarily be due to convergence to the solution; other reasons may be errors in input, inefficient use of the program by setting the dimension of the program to 1, or exceeding the iteration limit.

Some minor changes were made in the routines obtained from Jones. The Markrep routines called for IMSL routine LEQT1F to be used as a linear equation solver using Gaussian elimination (Crout algorithm) with equilibration and partial pivoting. The IMSL library was not available so a routine based on the Cholesky method was used instead (James,et.al., 1977). The subroutines for calculating -2 ln(likelihood) were modified so that they checked the sign of the (1,1) element in the covariance array, which should always be positive, before attempting to take the square root of that element (dimensioned real).

According to Jones, a negative sign could be caused by roundoff error and could be alleviated by inserting a small observational error into the reading. Consideration of observational error was available in the routines, but not used in order to contain the number of models. The program stopped prematurely on 6 of 24 data files before this check was implemented. Roundoff error was also observed in one test case where the values were small and many were missing, in a pattern of 15 present, 60 missing. A solution was adequately obtained after doubling the values in the file and processing. The non-linear optimization routine also was modified to check the sign of numbers before taking the square root. No case was observed where this error occurred, but the check was inserted as a precaution.

The output of the optimization routine was also modified. Originally, the program had three levels of messages which would print out varying levels of information as the program progressed, none of which would print out no information and also allow the model to run an ARMA(0,1) or ARMA(1,0) model. Since the program could generate sizable amounts of monitoring data while running 40 models, the desired change was made.

THEORY OF THE ARMA PROCESS

The following is the theoretical basis for the subroutine set Markrep, which calculates -2 ln(likelihood), as given by Jones(1980,1985a), and is included here for the benefit of the reader. An autoregressive moving average process with an order of p,q (ARMA(p,q)) and a zero mean can be expressed as

$$x_i = \sum_{k=1}^{p} \alpha_k x_{t-k} + \varepsilon_t + \sum_{k=1}^{q} \beta_k \varepsilon_{t-k} \qquad [1]$$

The first summation term represents the autoregressive part where the present

x is dependent on p previous x's. The second summation term determines the contribution that the past shocks make to the present value of x; only the past q values are considered, hence the model is referred to as ARMA(p,q). The ε_t term is a part of the model no matter what degree of q is used. The "real x" is considered to be specified within a certain range which is indicated by the magnitude of ε_t. The random noise is the only input from the environment into the system. The value has a defined mean, in this case 0, with the true value distributed about the mean. Thus even an ARMA(0,0) model would not always have a value of 0; the mean of the data would be 0 and the numbers would be distributed within a defined variance.

An assumption is made that the process is stationary; in other words, if the process is sampled from time t to t+k and then sampled at time t+m to t+n, the mean will be the same and the variance of the shock noise will be the same. The values of k, m, and n are arbitrary and the value of the mean is not necessarily zero for the definition of stationarity to be met. The assumption of stationarity means that the roots of

$$1 - \sum_{k=1}^{p} \alpha_k z^k = 0 \qquad [2]$$

must lie outside of the unit circle. The coefficients of the x_{t-k} (equation (1)) not have to lie between -1 and 1 to meet this condition. For example, the roots of the equation could be 2 and 5/4, both of which lie outside of the unit circle; equation (2) would then be

$$1 - 1.3z + .4z^2 = 0$$

The equation must also be invertible; that is, the equation below must have roots outside the unit circle.

$$1 + \sum_{k=1}^{q} \beta_k z^k = 0 \qquad [3]$$

Without this constraint, the influence of the random shocks would continue to grow as time progressed and the uniqueness of the parameters would be lost.

The state of the process in Akaike's Markovian representation (Akaike,1974) is defined as a column vector, **Z**, with a length of m, where

$$m = \text{Max}(p,q+1) \qquad [4]$$

$$\mathbf{Z}(t) = \begin{bmatrix} x(t|t) \\ x(t+1|t) \\ \vdots \\ x(t+m-1|t) \end{bmatrix} \qquad [5]$$

where x(t+j|t) is the prediction j steps ahead when given the x values up to the time t. Hence, x(t|t) is simply the value x_t. Rewriting equation (1) for a one-step prediction using this terminology gives

$$x(t+1|t) = \sum_{k=1}^{p} \alpha_k x_{t+1-k} + \sum_{k=1}^{q} \beta_k \varepsilon_{t+1-k} \qquad [6]$$

Expanding to a j-step prediction uses the previous predictions and yields

$$x(t+j|t) = \sum_{k=1}^{j-1} \alpha_k x(t+j-k|t) + \sum_{k=j}^{p} \alpha_k x_{t+j-k} + \sum_{k=j}^{q} \beta_k \varepsilon_{t+j-k} \qquad [7]$$

If the indices are beyond their proper range, the summations concerned are eliminated. Updating equation (7) to time t+1, it becomes

$$x(t+j|t+1) = \sum_{k=1}^{j-2} \alpha_k x(t+j-k|t+1) + \sum_{k=j-1}^{p} \alpha_k x_{t+j-k} + \sum_{k=j-1}^{q} \beta_k \varepsilon_{t+j-k} \qquad [8]$$

Subtracting equation (7) from (8) gives a recursion which involves only the random input at time t+1:

$$x(t+j|t+1) - x(t+j|t) = \sum_{k=1}^{j-1} \alpha_k [x(t+j-k|t+1) - x(t+j-k|t)] + \beta_{j-1}\varepsilon_{t+1} \quad [9]$$

If the term in brackets is redefined,

$$x(t+j|t+1) - x(t+j|t) = g_j\varepsilon_{t+1} \quad [10]$$

where g_j is some, as yet undefined, constant. Equation (9) can be rewritten as

$$x(t+j|t+1) = x(t+j|t) + \left[\beta_{j-1} + \sum_{k=1}^{j-1} \alpha_k g_{j-k}\right]\varepsilon_{t+1} \quad [11]$$

The quantity in brackets may be combined into one general variable called g, where

$$g_1 = 1 \quad [12]$$

$$g_j = \beta_{j-1} + \sum_{k=1}^{j-1} \alpha_k g_{j-k} \quad [13]$$

and $\beta_j = 0$ for $j > q$. Equation (11) can then be written more compactly as

$$x(t+j|t+1) = x(t+j|t) + g_j\varepsilon_{t+1} \quad [14]$$

with the final element in the state vector written as

$$x(t+m|t+1) = \sum_{k=1}^{p} \alpha_k x(t+m-k|t) + g_m\varepsilon_{t+1} \quad [15]$$

The autoregressive-moving average (ARMA) model can be described in a recursive fashion by using the state space framework. As an example, the technique is shown for a first-order autoregression and later generalized to a higher-order model. The equation for the ARMA(1,0) model consists of:

$$x(t+1) = ax(t) + \varepsilon(t) \qquad [16]$$

where x(t) is the state at time t, assuming zero mean, a is a value representative of the state transition matrix (For this first-order process the state transition matrix is a scalar.), and $\varepsilon(t)$ is a random shock with a variance of σ^2. If the process is observed with error, the observation equation becomes

$$y(t) = x(t) + v(t) \qquad [17]$$

where x(t) is the "true" process, v(t) is a white noise process with a variance R, and y(t) is the process for which values are actually obtained. This modification of (16) is equivalent to an ARMA(1,1) process since y(t+1) now depends on the previous value at (t) and an error in addition to a random excitation. The variance of this estimated state is

$$P(t+1|t) = E\{[x(t+1) - x(t+1|t)]^2\} \qquad [18]$$

At the beginning of a zero-mean process, the best estimate of the state is zero:

$$x(0|0) = 0 \qquad [19]$$

The variance of the process at the beginning is best estimated as

$$P(0|0) = \frac{\sigma^2}{1 - a^2} \qquad [20]$$

This is the variance that would be expected from a no-skills forecast. For the special case of first-order autoregression, the recursion proceeds as follows:

(a) Make a one-step forecast

$$x(t+1|t) = ax(t|t). \qquad [21]$$

(b) Calculate its variance

$$P(t+1|t) = a^2P(t|t) + \sigma^2. \qquad [22]$$

(c) Predict the next observation by

$$y(t+1|t) = x(t+1|t). \qquad [23]$$

(d) When the next observation is available, calculate the residual or "innovation"

$$I(t+1) = y(t+1) - y(t+1|t) \qquad [24]$$

(e) The variance of the innovation is

$$V(t+1) = P(t+1|t) + R \qquad [25]$$

(f) If the errors are Gaussian, the contribution to -2 ln(likelihood) from this step of the recursion is

$$\ln(V(t+1) + [I(t+1)]^2 / V(t+1). \qquad [26]$$

(g) The state is updated by

$$x(t+1|t+1) = x(t+1|t) + P(t+1|t)I(t+1) / V(t+1). \qquad [27]$$

This equation can also be written as a weighted average of the old estimate and the new observation, with the weighting inversely proportional to the variances, giving

$$x(t+1|t+1) = \left[\frac{x(t+1|t)}{P(t+1|t)} + \frac{y(t+1)}{R}\right] / \left[\frac{1}{P(t+1|t)} + \frac{1}{R}\right] \qquad [28]$$

(h) Finally the variance is updated by

$$P(t+1|t+1) = P(t+1|t) - [P(t+1|t)]^2 / V(t+1) \qquad [29]$$

The -2 ln(likelihood) function is calculated for assumed values of a, σ^2, and R by summing (26) over all the data points:

$$-2 \ln(\text{likelihood}) = \Sigma \{\ln[V(t+1)] + [I(t+1)]^2 / V(t+1)\} \quad [30]$$

A nonlinear optimization routine then varies the values of the parameters until the minimum value for -2 ln(likelihood) is found. When data points are missing, only steps (a) and (b), which make a prediction and estimate its variance, are calculated and then the algorithm returns to step (a). Thus, the above procedure gives the exact likelihood for the available data even though observations are missing.

Most times, the variance σ^2 is not known; it can be removed from the estimation problem by differentiating (30) with respect to σ^2 and setting the result equal to zero (Jones,1980).

$$\sigma^2 = \frac{1}{n} \sum_{i=1}^{n} I(i)^2 / V(i) \quad [31]$$

Substituting this result back into equation (30) gives the function to be minimized.

$$l = \sum_{i=1}^{n} \ln V_i + n \ln \sum_{i=1}^{n} [I(t+1)]^2 / V_i \quad [32]$$

Akaike's Information Criterium (AIC) is then computed by

$$AIC = -2 \ln(\text{likelihood}) + 2 \quad [33]$$

Generalizing to a higher-order model necessitates the use of two equations when using the Kalman state space model. The general case uses matrices instead of scalars. The first equation is the state equation, expressed in matrix form as

$$\begin{bmatrix} x(t+1|t+1) \\ x(t+2|t+1) \\ \vdots \\ x(t+m|t+1) \end{bmatrix} = \begin{bmatrix} 0 & 1 & 0 & \cdots & 0 \\ 0 & 0 & 1 & \cdots & 0 \\ & & \vdots & & \\ & & \vdots & & \\ \alpha_m & \cdots & & \alpha_2 & \alpha_1 \end{bmatrix} \times \begin{bmatrix} x(t|t) \\ x(t+1|t) \\ \vdots \\ x(t+m-1|t) \end{bmatrix} + \begin{bmatrix} 1 \\ g_2 \\ \vdots \\ g_m \end{bmatrix} \varepsilon_{t+1} \qquad [34]$$

The state equation can be written as

$$\mathbf{X}(t+1) = \Phi(t)\mathbf{X}(t) + \mathbf{U}(t) \qquad [35]$$

where $\mathbf{X}(t)$ is the state vector, $\Phi(t)$ is the state transition matrix, and $\mathbf{U}(t)$ is a vector of the random plant noise with a covariance matrix $Q(t)$. The $g\varepsilon$ term (see equation (10)) corresponds to the $\mathbf{U}(t)$ term. The second equation in the state-space representation is the observational equation

$$\mathbf{Y}(t) = \mathbf{M}(t)\mathbf{X}(t) + \mathbf{v}(t) \qquad [36]$$

where $\mathbf{M}(t)$ is the matrix showing which linear combinations of the state vector are observed. The observation vector $\mathbf{Y}(t)$ does not have to be the same length as the $\mathbf{X}(t)$ vector. The random observational error vector $\mathbf{v}(t)$ has the covariance matrix $\mathbf{R}(t)$. The algorithm for the general case is:

(a) Make a one-step forecast by

$$\mathbf{X}(t+1|t) = \Phi(t)\mathbf{X}(t|t). \qquad [37]$$

(b) Calculate its covariance by

$$\mathbf{P}(t+1|t) = \Phi(t)\mathbf{P}(t|t)[\Phi(t)]' + \mathbf{Q}(t). \qquad [38]$$

(c) Predict the next observation vector by

$$\mathbf{Y}(t+1|t) = \mathbf{M}(t+1)\mathbf{X}(t+1|t). \qquad [39]$$

(d) When the next observation is available, calculate the innovation vector

$$\mathbf{I}(t+1) = \mathbf{Y}(t+1) - \mathbf{Y}(t+1|t) \qquad [40]$$

(e) The covariance matrix of the innovation vector is

$$\mathbf{V}(t+1) = \mathbf{M}(t+1)\mathbf{P}(t+1|t)[\mathbf{M}(t+1)]' + \mathbf{R}(t+1) \qquad [41]$$

(f) The contribution to -2 ln(likelihood) is

$$\ln|\mathbf{V}(t+1)| + [\mathbf{I}(t+1)]'[\mathbf{V}(t+1)]^{-1}\mathbf{I}(t+1) \qquad [42]$$

where $|\mathbf{V}(t+1)|$ is the determinant of the covariance matrix.

(g) The state is updated by

$$\mathbf{X}(t+1|t+1) = \mathbf{X}(t+1|t) + \mathbf{P}(t+1|t)[\mathbf{M}(t+1)]'[\mathbf{V}(t+1)]^{-1}\mathbf{I}(t+1). \qquad [43]$$

(h) Finally, the state covariance matrix is updated by

$$\mathbf{P}(t+1|t+1) = \mathbf{P}(t+1|t) - \mathbf{P}(t+1|t)[\mathbf{M}(t)]'[\mathbf{V}(t+1)]^{-1}\mathbf{M}(t)\mathbf{P}(t+1|t). \qquad [44]$$

The AIC number is computed by an expansion of equation (33):

$$\text{AIC} = -2\ \ln(\text{likelihood}) + 2(p + q) \qquad [45]$$

The above procedure proceeds satisfactorily as long as the coefficients show no inclination to pass the boundary as established in equations (2) and (3). If they wander close to the boundary while being evaluated by the optimization program, the stability and invertibility of the model may be threatened. Therefore, Jones' subroutines ensure that the model stays within its limits by reparameterizing in terms of the partial autoregressive coefficients, a_n, so that the a's can be constrained to lie between -1 and +1 by the transformation

$$a_n = [1 - \exp(-u_n)] \ / \ [1 + \exp(-u_n)] \qquad [46]$$

The α's can then be calculated using the Levinson-Durbin recursion, for n=1,...,p. The n's in equations (45-48) increment by 1, up to and including the value p, each time the recursion is done.

$$\alpha_n = a_n \qquad [47]$$

If n = 1, the recursion is complete and begins again at equation (45) with n = 2. When n equals 2 or more, a_m is calculated, where m = 1,...,n-1

$$a_m = \alpha_m - a_n\alpha_{n-m} \qquad [48]$$

The α_i variables are then reset for the next recursion.

$$\alpha_i = a_i \qquad i=1,\ldots,n-1 \qquad [49]$$

If n ≠ p, the recursion begins again at equation (46); otherwise the autoregressive (α_i) coefficients have been found when n = p.

The moving average coefficients can similarly be transformed in the recursion (equations (50-53) for n = 1,...,q.

$$b_n = [1 - \exp(-w_n)] \;/\; [1 + \exp(-w_n)], \qquad [50]$$

The newest β's are initialized for the current process by

$$\beta_n = b_n \qquad [51]$$

with the next value for b_n, when n > 1, calculated by

$$b_m = \beta_m + b_n\beta_m \qquad m = 1,2,\ldots,n-1 \qquad [52]$$

As in the autoregressive case, $\beta_1 = b_1$ when n = 1. The β values are updated by

$$\beta_i = b_i \qquad i = 1,\ldots,n-1 \qquad [53]$$

and the process continues at equation (50) until n = q.

When observation error is included in the model, a transformation can be used to ensure a nonnegative estimate for the observational error variance.

$$R = s^2 \text{ or } R = e^s \qquad [54]$$

Now, the optimization routine can safely be run using the transformed variables

$$u_k,\ k = 1,\ldots,p$$

$$w_k,\ k = 1,\ldots,q$$

$$s$$

while the likelihood routine uses the untransformed variables of the α's and the β's.

RESULTS

The following models (Table 1) were selected for each data file by the criteria of AIC value, number of parameters, and suitability to the present case. A pattern to simulate the data in each file can be generated by using a slightly modified version of equation (1). Since a zero mean was used in that equation, the data simulation series, y, requires the mean x value to be added to the x_t value.

$$x_t = +\alpha_1 x_{t-1} + \alpha_2 x_{t-2} + \cdots + \alpha_p x_{t-p}$$

$$+\beta_1 \varepsilon_{t-1} + \beta_2 \varepsilon_{t-2} + \cdots + \beta_q \varepsilon_{t-q} + \varepsilon_t$$

$$y_t = x_t + \bar{x} \qquad [55]$$

The α's and β's are given in the table below, as is the mean. The ε's are generated from a gaussian random number generator with a standard deviation given by the estimated error deviation in the table. For test files, the recursive processes can be started by generating q gaussian random noises and initializing p x variables to zero. The process then generates numbers. The first few hundred values are not recorded so as to avoid the effects of the initial zeros. Any subsequent values can be collected and used to simulate the data in the original file. A FORTRAN program to regenerate the data series is given Appendix D.

Table 1. Models from the data files

Loc.	Operation	Mean (kW)	Est Err Dev	ARMA (p,q)	Model Coefficients α_1	α_2	α_3	α_4	α_5	α_6	β_1	β_2	β_3	β_4	β_5
1A	6.5m Drill	28.229	.994	3,5	.604	.089	.150				.115	-.092	-.092	.115	1.000
1B	6.5m Drill	29.403	1.367	4,4	.348	1.497	-.131	-.726			.042	-1.915	.042	1.000	
2A	8.1m Drill	32.335	1.674	4,5	.130	1.645	.132	-.972			1.048	-1.856	-1.856	1.048	1.000
2B	8.1m Drill	39.703	1.154	3,5	.321	-.325	.975				.553	1.056	-.752	-.360	-.922
3B	NH3 Application	78.803	1.799	5,4	2.567	-1.693	-.967	1.641	-.574		-2.000	0.000	2.000	-1.000	
4B	5.5m Chisel	79.721	3.695	4,5	.090	-.694	.090	.288			.970	1.868	1.868	.970	1.000
6A	9.1m Disk	69.395	1.687	5,5	.739	1.646	-.978	-1.058	.627		1.000	-2.000	-2.000	1.000	1.000
6B	9.1m Disk	56.706	1.086	6,4	-1.924	-.562	1.398	.949	-.269	-.353	4.000	6.000	4.000	1.000	
7A1	6.1m Disk/ Sp. Tooth	65.852	1.354	5,4	-1.993	-.606	1.431	1.366	.403		4.000	6.000	4.000	1.000	
7A2	Drag/Harrow	49.676	.729	2,5	1.230	-.976					-.805	1.010	1.010	-.805	1.000
7B1	6.1m Disk/ Sp. Tooth	69.502	2.223	5,5	1.582	-.806	.273	.426	-.494		-.688	-.227	-.227	-.688	1.000
7B2	Drag/Harrow	50.115	.965	4,3	3.248	-3.982	2.193	-.464			-2.988	2.977	-.988		
8A	6.7m Disk	69.070	1.826	5,5	-.744	.590	1.098	.165	-.558		2.247	1.389	-1.389	-2.247	-1.000
8B	6.7m Disk	66.083	.832	4,5	1.706	-1.207	.044	.403			-1.362	.965	.965	-1.362	1.000
8BL0	6.7m Disk	39.801	1.790	4,5	.107	1.736	.099	-.968			1.029	-1.913	-1.913	1.029	1.000
9A	5.5m Disk	65.736	2.470	4,4	3.531	-4.998	3.331	-.893			-3.999	5.998	-3.998	1.000	
	Alternate	65.736	2.775	5,5	-.278	1.675	.326	-.948	.198		.882	-1.882	-1.882	.882	1.000
9B	5.5m Disk	75.359	.923	6,4	-1.909	-.318	2.099	1.636	-.093	-.416	4.000	6.000	4.000	1.000	
9B2	9.8m Field Cult.	62.909	2.164	6,4	-2.176	-1.473	.422	1.350	1.088	.451	3.484	4.996	3.484	1.000	
9BH1	5.5m Disk	81.309	1.991	3,4	.972	.978	-.955				-.003	-1.858	-.003	1.000	
9BL0	5.5m Disk	55.541	2.704	5,5	-1.833	-.376	1.487	1.318	.403		3.091	2.363	-1.456	-2.637	-.909
10A	6.1m Disk	77.713	2.882	6,3	-1.689	-.508	.800	.448	-.254	-.300	3.000	3.000	1.000		
10B	6.1m Disk	88.341	3.311	4,3	-1.213	.501	1.026	.178			3.000	3.000	1.000		
10B2	9.8m Field Cult. w/ NH3	89.118	2.691	6,4	.882	1.343	-1.078	-.785	.723	-.142	0.000	-2.000	0.000	1.000	
	Alternate	89.118	2.990	3,5	.270	.199	.172				.573	.453	.453	.573	1.000
10B3	9.8m Field Cult.	96.334	3.256	5,5	.733	1.454	-1.053	-.907	.767		1.025	-1.926	-1.928	1.025	1.000

DISCUSSION

Spectral density was considered as an analysis technique in the hope that the data would show distinct variances at certain frequencies. One author, Wendenborn(1966), showed the recovery of both the original amplitude and frequency of three sine functions which made up a test series. The procedure worked for that series, but did not give consistent results for other series. An attempt at relating the amplitude of known sine curves to their peaks on the spectral density graph as obtained by the DQSE method by regression as a function of original amplitude, length of the time series, and frequency of the original curve was not successful. In light of the unpredictable effects of the beginning and end of the fine data, the attempt was abandoned. An attempt to follow the procedure used by Cryer and Nawrocki (1976) was impossible because the original tractor was no longer available.

The models were obtained by ranking 40 ARMA(p,q) models. The values of p ranged from 0 to 6 and the values of q from 0 to 5, with the sum of p and q less than or equal to 10, giving models from ARMA(0,1) to ARMA(5,5), and ARMA(6,0) to ARMA(6,4). The parameters for the models were selected by a computer program according to the the lowest -2 ln(likelihood). The values of AIC for each model were calculated from the likelihood value and the number of parameters and the models were ranked by ascending order of AIC. For each data file, the models with the lowest AIC numbers were considered in the selection of the best model of that data. To test each model, a series was generated by setting the first p variables to zero and generating q random noises. Values for x were then recursively generated to check the suitability of these models. The first 300 values of the series were discarded so as to

eliminate the effect of the initial zeroes. Subsequent values were then examined for similarity to the existing parts of the data file.

For some of the models that were considered, but not chosen, the generated series differed from the original, likely because the solution calculated by the optimization routine was approximate due to nonlinearity of the likelihood function near the optimum point. These approximate solutions often were rated among the best by AIC number and usually gave reasonable results so these models were considered as possibilities. In a few cases, the regenerated series oscillated through a much wider power range than was possible or was unreasonable, with ridiculously low power levels, for the tractor. Another reason for rejection was the occurrence of many values over the power rating of the tractor. This happened only when the mean power level was high. While some of these values would be expected to occur from the statistical standpoint from the properties of gaussian distribution, for practical implementation, they would be undesirable. The third reason for rejecting a model was observation of repetitive sharp changes in load level. Although some of these sharp increments were observed in the data, for some numbers generated by the models, the changes were large and frequent; at times, changes of ±20 kW were observed to occur sequentially. Despite instances where the parameters did not adequately fit the data, no cases were observed where the sequence diverged radically from the mean and never changed sign again; all the tested models oscillated about a mean of approximately zero.

The models that remained under consideration after checking the regenerated series were then rated by the closeness of the AIC numbers and the estimated error variance. If several models displayed similar AIC and EEV values, the simplest model was chosen. The definition of "close" was changed

from the guideline used by Jones. The reason for this was the greater value of the likelihood from the data files used in this analysis as compared to that of Jones'. If the models appeared to give the same type of values, with widely-differing AIC values, the model with the lowest AIC value was chosen. Some data files (9a and 10b2) give highly cyclical patterns with the "best" choice according to AIC and the other considerations. While the individual increments are not excessive, the series as a whole appears to be more cyclical than the available data. Thus, alternate models are offered for consideration.

The complexity of the models is perhaps related to the amount of missing data. In a test run with data generated from a known AR(3) process, the AIC number correctly predicted the model for the cases which used a complete data set and a pattern of 15 values followed by 1 missing. The AR(3) model was not selected as the top model for the case of 15 present followed by 5 missing or in the case of 15 present followed by 60 missing, as in the data files. In the last two cases, the parameters were correct for the AR(3) model, but the AIC number showed that this model was not the most probable. The "top" models were the more complex models.

As with all modeling procedures, roundoff error in the model-fitting routine is a concern. Such a problem was encountered in 6 out of 960 models. According to Jones, this could be remedied by inserting a small value for observational error into the program, which has the option to consider values read with error. Roundoff error was also noted when using a file of small test values with a pattern of 15 present, 60 missing. When the complete file was used, the problem did not occur. The problem was alleviated by multiplying the file by 2; the solution was adequately obtained.

A small section of data and the regenerated series is shown in Appendix C for each data sample. On some of the graphs of actual data, a large power dip can be noted. This occurs when the tractor makes a turn since the speed is constant and the rack signal, indicating torque, drops sharply. On the graphs, two other items of note are that the data displayed is only a small portion of that available for analysis and on the regenerated series, if the power value exceeds 115 kW, as is possible according to a gaussian distribution, the graphed value was 115 kW, as it would be limited when actually used on the dynamometer.

The resulting models are unique for each field data file, but some general characteristics can be noted. The difference between models reflects the variability between agricultural fields and operating practices. The drills show a low mean. Both 1a and 1b show only small deviations from the general trend, which is relatively flat. The 2a and 2b series show a rougher pattern, particularly 2a. While some these changes may appear to be excessive, the actual does show some large steps. Sample 1a is chosed to represent the drills since the actual and regenerated series are quite similar and resemble the rest of the samples.

The series for a chisel (location 4b) is quite rough. This is expected since this tool is a primary tillage tool with a fracturing mode of soil fracture as opposed to cutting by a disk. The mean level is relatively high (79.7 kW) and the series show power fluctuations reaching almost to the maximum power level.

The drag/harrow combination (locations 7a2 and 7b2) showed a smooth pattern. The simulated series for 7b2 does not show the sharp peaks that some of

the data shows. The drag, as recorded by Blumanhourst, was an old truck frame. This combination was not hooked solidly to the tractor and so would tend to jerk at the corners. The smoothness of the series is expected since this tool combination was being used to level and smooth the seedbed under a center pivot irrigation system. The operation can be represented by location 7a2.

The disk/springtooth combination (locations 7a1 and 7b1) shows a pattern of small oscillations about the long-term trend. The data for series 7 shows the effect of turns with this operator. The combination of tools does not appear to be distinct from the disk alone, given the variability of disk samples. The series are quite similar, but since 7a1 avoids the apparent cyclical tendency of 7b1, an ordinary field without definite slopes can be represented by the 7a1 series.

The field cultivator (locations 9b2 , 10b2, and 10b3) provide the opportunity to observe the differences between operators and fields. Location 9b2 had an actual mean of 62.9 kW, and 10b2 is 89.1 kW, while at 10b3 the mean was 96.3 kW. As a result, 10b3 shows a series with some oscillations near the maximum level while 9b2 never approaches these levels. For 9b2, the simulated series varies from the mean with no evident pattern while 10b2 and 10b3 have some cyclical tendencies. At location 10, the apparent small field size, with the resulting frequent drops in power levels at the turns, may have contributed to a cyclical tendency and large step size between the proposed patterns for 10b2 and 10b3 while the data shows a finer variation. Thus, 9b2 is the best choice to represent a field cultivator. At 10b2, the alternate choice agrees more with the series for 3b, which is NH3 application, in that the variations from one time increment to the next are smaller. The ground

surface would be expected to be fairly even when applying anhydrous ammonia since the soil surface needs to be fine enough so the ammonia does not escape from the soil.

The disk tool has the largest number of samples and also the largest variation between the eleven samples. Four sizes of disks are represented. 5.5m, 6.1m, 6.7m, and 9.1m. The mean power levels range from 39.8 kW to 88.3 kW. Most samples and regenerated series show a moderate variation from one increment to the next. The long term trend for some is cyclical (6a or 9a, alt.). For others, the trend is flat (8a or 8b). Size of tool does not appear to be a determining factor for the variation; the EED for 9b (5.5m disk) is .923 kW, for 6b (9.1m disk) it is 1.086 kW, and for 8b (6.7m disk) the deviation is .832 kW. There is also variation between samples for the same location. For location 8, 8a has 1.826 kW EED, 8b has .832 kW, and 8blo has 1.790 kW, yet the means for 8a and 8b are close. Given the variability between each series, a "typical" disk pattern is difficult to select. In the interests of providing a pattern intermediate between the smooth drag/harrow and the chisel, which most of the samples appear to be, 8a is selected because it contains both small incremental changes and sharp adjustments in power usage.

CONCLUSIONS

1. The results of this study are a model of each of the data samples. The models were obtained using the ARMA(p,q) approach in which the value at time t is dependent on p past values, q past random noises, and a random noise at time t.

2. Generalizations about the models are possible. Drills and the drag/harrow combinations have a relatively smooth pattern. The chisel showed a rough pattern. The field cultivator has a roughness less than the chisel, but more than the disk. The disk samples showed a variety of

patterns, but the power loading pattern for each model was generally between the drill and chisel in terms of roughness. The disk/springtooth combination was not noticeably different from the disk. The variation when NH3 was applied was apt to be small between successive time increments.

SUMMARY

The autoregressive moving average approach was used to determine a model for each data sample which could recursively regenerate the represented series of power loading variations for a tractor. The method accommodated evenly-spaced data with missing values by adjusting coefficients for the past values through a nonlinear optimization routine until the minimum value of -2 ln(likelihood) was reached. Spectral density was also considered, but was rejected due to the difficulty of definitely correlating the amplitude of known sine curves to the values on the power spectral density graph.

The models of power loading variation obtained for the different tillage tools show that the drill and drag/harrow have fairly small variations between time increments. The disk samples generally show a moderately rougher pattern, with no noticeable difference when a springtooth is attached. The chisel appears to be the roughest series and the field cultivator shows slightly smaller deviations. When NH3 is applied, the increments from step to step are small although the general trend varies.

SUGGESTIONS FOR FURTHER RESEARCH

Anyone wishing to do work on the time series of tractor power variations with various tillage implements, or any other time series, would find it beneficial to begin with a series with no missing values at evenly-spaced

intervals. This would allow the use of conventional theory for which means of analysis have been well-established.

The time series analysis in this study was done on field data without quantifying the effects of different variables on the power level. A careful analysis could lead to an even better representation of power usage during tillage. Possible areas to investigate include the following:

1. The effect of different soil types on the power usage pattern. Soils of varying composition could possibly yield distinct patterns.

2. The differences between the sequences derived from specific tillage implements.

3. The impact on the regenerated series of the actual power drops due to turns. When the tractor makes a turn, the power level drops sharply and then rises sharply. The regenerated series was not able to show these sharp drops.

4. Simulation of hills with the possibility of adding or removing slopes when desired.

BIBLIOGRAPHY

Akaike, Hirotugu. 1974. Markovian representation of stochastic processes and its application to the analysis of autoregressive moving-average processes. Annals of the Institute of Mathematics 26: 363-387.

American Society of Agricultural Engineers. 1983. Agricultural engineers yearbook of standards. St. Joseph, MI. The Society.

Bekker, M. G. 1969. Introduction to terrain-vehicle systems. Ann Arbor. The University of Michigan Press. pp. 181-191.

Blackman, R. B. and J. W. Tukey. 1958. The measurement of power spectra from the point of view of communications engineering. New York. Dover Publication, Inc.

Blumanhourst, M. B. 1984. Evaluation of a gear selection aid for fuel efficient tractor operation. Unpublished Thesis. KSU Library. Manhattan, KS.

Blumanhourst, Michael B., et al. 1984. Gear selection aid field evaluation. ASAE paper No. MCR 84-105.

Box, George E. P. and Gwilym M. Jenkins. 1976. Time series analysis: forecasting and control. Revised Ed. San Francisco. Holden-Day.

Boyce, William E. and Richard C. DiPrima. 1977. Elementary differential equations and boundary value problems. 3rd ed. New York. John Wiley & Sons. pp. 476-478.

Chaka, Ronald J. 1978. The design and development of a highway speed road profiler. SAE paper 780064.

Cryer, B. W. and P. E. Nawrocki. 1976. A road simulation system for heavy duty vehicles. SAE paper 760361.

Grisso, R. D. and John V. Perumpral. 1985. Review of models for predicting performance of narrow tillage tool. Transactions of the ASAE 28(4): 1062-1067.

Harvey, A. C. and R. G. Pierse. 1984. Estimating missing observations in economic time series. Journal of the American Statistical Association. 79(385): 125-131.

International Organization for Standardization. 1983. Agricultural machinery: international standards for tractors and machinery for agriculture and forestry. 1st. ed. Gene've. The Organization.

James, M. L., G. M. Smith, and J. C. Wolford. 1977. Applied numerical methods for digital computation with FORTRAN and CSMP. 2nd Ed. New York. Harper & Row, Publishers, Inc.

Jones, R. H. 1962. Spectral estimates and their distributions, Skandinavisk Aktuarietidskrift, Part I and Part II, pp. 39-153.

_____ 1978. Markrep. Computer program. University of Colorado Medical Center, Denver, CO.

_____ 1980. Maximum likelihood fitting of ARMA models to time series with missing observations. Technometrics 22(3): 389-395.

_____ 1985a. Time series analysis - time domain. Probability, statics, and decision making in the atmospheric sciences. Eds. Allan H. Murphy and Richard W. Katz. Boulder. Westview Press. Ch. 6, pp. 223-259.

_____ 1985b. Time series with unequally spaced data. Handbook of statistics. Eds. E. J. Hannan, P. R. Krishnaiah, M. M. Rao. New York. Elsevier Science Publishers B. V. pp. 157-177.

Leviticus, Louis I. and Jose' F. Reyes. 1985. Tractor performance on concrete. Transactions of the ASAE 28(5): 1425-1429.

Marquardt, D. W. and S. K. Acuff. 1982. Direct quadratic spectrum estimation from unequally spaced data. Applied time series analysis. Eds. O. D. Anderson and M. R. Perryman. Amsterdam. North Holland Publishing Co. pp. 199-227.

_____ 1984. Direct quadratic spectrum estimation with irregularly spaced data. Time series analysis of irregularly observed data: proceedings of a symposium held at Texas A & M University, College Station, Texas February 10-13, 1983. Ed. Emanuel Parzen. New York. Springer-Verlag. pp. 211-223.

Masry, Elias. 1984. Spectral and probability density estimation from irregularly observed data. Time series analysis of irregularly observed data: proceedings of a symposium held at Texas A & M University, College Station, Texas February 10-13, 1983. Ed. Emanuel Parzen. New York. Springer-Verlag. pp. 224-250.

National Center for Atmospheric Research. An unconstrained non-linear optimization solver. Computer program. Boulder, CO.

Otnes, Robert K. and Loren Enochson. 1972. Digital time series analysis. New York. John Wiley & Sons, Inc.

Parzen, Emanuel, Ed. 1984. Time series analysis of irregularly observed data: proceedings of a symposium held at Texas A & M University, College Station, Texas February 10-13, 1983. New York. Springer-Verlag.

Society of Automotive Engineers. 1985. SAE handbook. Vols. 3 and 4. Warrendale, PA. The Society.

Walls, James H., John C. Houbolt, and Harry Press. 1954. Some measurements and power spectra of runway roughness. Technical Note 3305. National Advisory Committee for Aeronautics.

Wendenborn, J. G. 1966. The irregularities of farm roads and fields as sources of farm vehicle vibrations. Journal of terramechanics 3(3): 9-40.

Whelpley, Thomas D. 1973. Simulation of farm tractor field loading through laboratory programmed control. SAE 730820.

Wonacott, Thomas H. 1961. Spectral analysis combining a Bartlett window with an associated inner window. Technometrics 3(2): 235-243.

APPENDIX A - CONTINUOUS AND DISCRETE SPECTRA

Continuous Spectra

The spectral density method of analyzing time series relates the autocovariance to the frequency. A plot of power spectral density against frequency shows whether a series is white noise, with a constant variance over all frequencies, or has a periodic tendency within a certain frequency range. The main sources for this presentation are Blackman and Tukey (1958) and Otnes and Enochson (1972). The theory can also be found in other sources dealing with time series analysis.

To begin with, let the time series x(t) be a simple sinusoid.

$$x(t) = \cos \omega t \qquad [1]$$

For simplicity, let ω be a nonnegative number. This series goes through one complete cycle, a period, in time T. The frequency, f, is the reciprocal of T and is measured in cycles/sec (hz). So the units cancel, ω is defined as the angular frequency (rad/sec). By definition, 2π radians equal a cycle so

$$\omega = 2\pi f \qquad [2]$$

Adding two more parameters, A and ϕ, called amplitude and phase, respectively, gives a more general equation

$$x(t) = A \cos(\omega t + \phi) \qquad [3]$$

A is the maximum amplitude from the mean value, in this case zero, and ϕ is the displacement of the sinusoid from the given time origin (the phase shift). For simplicity, A is a non-negative number. Any number of patterns can be created by changing the parameters in equation (3) and adding one or more sinusoids together. Most natural processes would be expected to contain more than one frequency. This new type of series is given by

$$x(t) = \sum_{i=1}^{n} A_i \cos(\omega_i t + \phi_i), \qquad -\infty < t < \infty \qquad [4]$$

The classic approach to the power spectral density as outlined by Blackman and Tukey (1958, pp.84-87) deals first with autocovariance. Let x(t) be some real function of time. If the mean of the function is 0 as time approaches time limit T

$$\lim_{T\to\infty} \frac{1}{T} \int_{-T/2}^{T/2} x(t)\, dt = 0 \qquad [5]$$

then the autocovariance function, R, of the process is defined as:

$$R(\tau) = \lim_{T\to\infty} \frac{1}{T} \int_{-T/2}^{T/2} x(t)\cdot x(t+\tau)\, dt \qquad [6]$$

The variable τ is a difference in time known as the time lag and is unrelated to ϕ. Where $R(\tau)$ is defined for a finite piece of a function, it is called the apparent autocovariance function. When τ is 0, a special case of the autocovariance function results, the variance function:

$$R(0) = \lim_{T\to\infty} \frac{1}{T} \int_{-T/2}^{T/2} [x(t)]^2\, dt \qquad [7]$$

This definition of variance is the same as the usual statistical definition since the function x(t) has the mean defined to be zero.

The spectral density function is the Fourier transform of the autocovariance density.

$$P(f) = \int_{-\infty}^{\infty} R(\tau)\cdot e^{-i\omega\tau} d\tau \qquad [8]$$

For a derivation of this as well as an explanation of the use of the word "power" to describe the spectrum, see Blackman and Tukey (pp.85-86). R(f) is the inverse Fourier transform of $P(\tau)$:

$$R(\tau) = \int_{-\infty}^{\infty} P(f)\, e^{i\omega\tau} df \qquad [9]$$

Even and odd functions have properties that can simplify an equation (Boyce and DiPrima, 1977). P(f) and $R(\tau)$ are even functions since $P(f) = P(-f)$ and $R(\tau) = R(-\tau)$.
Letting $g(\tau)$ be an even function as shown above,

$$\int_{-\infty}^{\infty} g(\tau)d\tau = \int_{0}^{\infty} g(\tau)d\tau + \int_{-\infty}^{0} g(\tau)d\tau$$

substituting $\tau = -s$ in the rightmost term,

$$= \int_{0}^{\infty} g(\tau)d(\tau) - \int_{\infty}^{0} g(s)\, ds$$

The - sign comes from the derivative of s [$g(s) = g(-s)$]. Inverting limits on the rightmost term adds another - sign, making the overall sign of the term positive.

$$= \int_{0}^{\infty} g(\tau)d\tau + \int_{0}^{\infty} g(s)ds$$

$$= 2 \int_0^{\infty} g(\tau)d\tau$$

The area in both integrals is the same and additive.

When $h(\tau)$ is an odd function, $h(-\tau) = -h(\tau)$ and the integration from $-\infty$ to $+\infty$ gives a result of zero.

$$\int_{-\infty}^{\infty} h(\tau)d\tau = \int_0^{\infty} h(\tau)d\tau + \int_{-\infty}^{0} h(\tau)d\tau$$

$$= \int_0^{\infty} h(\tau)d\tau + \int_{\infty}^{0} -h(s)(-ds)$$

$$= \int_0^{\infty} h(\tau)d\tau - \int_0^{\infty} h(s)ds = 0$$

The area in both integrals is the same, leading to an answer of 0.

Equation (8) can be rewritten as

$$P(f) = \int_{-\infty}^{\infty} R(\tau)[\cos\omega\tau - i \sin \omega\tau]d\tau \qquad [10]$$

The function cos $\omega\tau$ is even since $\cos(\omega\tau) = \cos(-\omega\tau)$. Multiplication of an even function by another even function yields an even function:
Let $g(\tau) = R(\tau)\cos(\omega\tau)$

$$g(-\tau) = R(-\tau)\cdot\cos(-\omega\tau)$$

$$= R(\tau)\cdot\cos(\omega\tau)$$

$$= g(\tau)$$

Multiplication of an even function by an odd function yields an odd function. The sin $(\omega\tau)$ is an odd function since $\sin(\omega\tau) = -\sin(\omega\tau)$.
Let $h(\tau) = R(\tau)\sin \omega\tau$

$$h(-\tau) = R(-\tau)\sin(-\omega\tau)$$

$$= R(\tau)[-\sin \omega\tau]$$

$$= -R(\tau)\sin \omega\tau$$

$$= -h(\tau)$$

Since the integral of an odd function $h(\tau)$ is zero, equation (10) can be simplified to the cosine transform of $R(\tau)$

$$P(f) = \int_{-\infty}^{\infty} R(\tau)\cos\ \omega\tau\ d\tau \quad \text{and} \quad R(\tau) = \int_{-\infty}^{\infty} P(f)\cos\ 2\pi f\tau\ df \qquad [11]$$

$$(2\pi f = \omega)$$

or even more simply as one-sided cosine transforms using the property of an even function:

$$P(f) = 2\int_{0}^{\infty} R(\tau)\cos\ \omega\tau\ d\tau \qquad [12]$$

$$R(\tau) = 2\int_{0}^{\infty} P(f)\cos\ 2\pi f\tau\ df \qquad [13]$$

For further discussion of the power spectral density, two more mathematical concepts will be helpful. One of these is known as the Dirac delta function. The delta function, $\delta(t-t_o)$ is introduced by formally identifying $f(t - t_o)dt$ with $dh(t - t_o)$ (Blackman and Tukey, 1958,p. 69) where $h(t - t_o)$ is Heavisides' step function

$$h(t - t_o) = 0, \quad t < t_o$$
$$h(t - t_o) = 1, \quad t < t_o$$

So if the time function is the delta function

$$G(t) = \delta(t-t_o),$$

the equivalent frequency function is

$$S(f) = e^{-i\omega t_o} \qquad [14]$$

The delta function is arbitrarily tall and narrow, yet has a unit area. Otnes and Enochson (1972, p.14) also give two functions derived from the delta function.

$$F^{-1}\left[\frac{\delta(f-f_o) + \delta(f+f_o)}{2}\right] = \cos\ 2\pi f_o t \qquad [15]$$

$$F^{-1}\left[\frac{\delta(f-f_o) - \delta(f+f_o)}{2j}\right] = \sin\ 2\pi f_o t \qquad [16]$$

Convolution, another important property, is the operational transform between the frequency and time domain that works as follows (Blackman and Tukey,1958, p.72): If $G(t) = G_1(t) \cdot G_2(t)$, and $S(f)$ is the frequency counterpart of $G(t)$, then the Fourier transform of $G(t)$ in terms of $G_1(t)$ and $G_2(t)$ is

$$S(f) = \int_{-\infty}^{\infty} G_1(t) \cdot G_2(t) \cdot e^{-i\omega t} dt \qquad [17]$$

$$= \int_{-\infty}^{\infty} G_1(t) \cdot \left[\int_{-\infty}^{\infty} S_2(\xi) \cdot e^{i2\pi\xi t} d\xi \right] \cdot e^{-i\omega t} dt, \qquad [18]$$

where $S_2(f)$ is the frequency domain equivalent of $G_2(t)$

$$= \int_{-\infty}^{\infty} \left[\int_{-\infty}^{\infty} G_1(t) \cdot e^{-i2\pi(f-\xi)t} dt \right] \cdot S_2(\xi) d\xi \qquad [19]$$

$$= \int_{-\infty}^{\infty} S_1(f-\xi) \cdot S_2(\xi) d\xi \qquad [20]$$

$S_1(f)$ and $S_2(f)$ are interchangeable in this operation, also written as

$$S(f) = S_1(f) * S_2(f) \qquad [21]$$

The "*" indicates the convolution operation. For the completeness of the transform operation, the process of going from multiplication in the frequency domain to convolution in the time domain is, given $S(f) = S_1(f) \cdot S_2(f)$,

$$G(t) = \int_{-\infty}^{\infty} G_1(\tau-\lambda) \cdot G_2(\lambda) d\lambda = G_1(t) * G_2(t) \qquad [22]$$

For the continuous domain, the limits of $+\infty$ to $-\infty$ work well, but in the real world of experiments, the data samples have a beginning and an end as well as a finite length. To deal with these difficulties, the idea of a "box-car function" is introduced, designated as $u_T(\tau)$.

$u_T(\tau) = 1 \quad |\tau| \leq T$
$u_T(\tau) = 0 \quad |\tau| > T$

Its Fourier transform is

$$U_T(f) = \int_{-\infty}^{\infty} u_T(t) e^{-i\omega t} dt$$

$$= \int_{-T}^{T} e^{-i\omega t} = \frac{2 \sin \omega T}{\omega} \qquad [23]$$

The infinite limited transform integral for the power spectrum can now be

written in terms of the boxcar function (Otnes and Enochson, 1972). The prime sign shows the variable is computed for the finite length rather than the infinite.

$$P'(f) = \int_{-\infty}^{\infty} u_T(\tau) \cdot R(\tau) \cdot e^{-i\omega\tau} d\tau \qquad [24]$$

As shown above in the convolution theorem, multiplication in the time domain corresponds to convolution in the frequency domain. Thus, equation (24) can be written as

$$P'_x(f) = P_x(f) * U_T(f) \qquad [25]$$

$$= \int_{-\infty}^{\infty} S(f_o) \cdot U_T(f-f_o) df_o \qquad [26]$$

Substituting for the $U_T(f-f_o)$ term (see Equation (23)) yields

$$P'_x(f) = \int_{-\infty}^{\infty} S_x(f_o)\, 2\, \frac{\sin\,[2\pi T(f-f_o)]}{2\pi(f-f_o)}\, df_o \qquad [27]$$

As can be seen, the frequency components are not dependent on one another and hence their contributions to the power spectrum are additive; each source contributes separately.

For an example (Otnes and Enochson, 1972, p.202), let the $R_x(\tau)$ function be the covariance of a cyclical batch of data:

$$R_x(\tau) = \frac{A^2}{2} \cos 2\pi f_o \tau \qquad [28]$$

Then, $R_x(f)\tau)$ corresponds to $P_x(f)$ in the frequency domain (see equation (15))

$$P_x(f) = \frac{A^2}{4} [\delta(f-f_o) + \delta(f+f_o)], \qquad [29]$$

which are delta functions centered at $-f_o$ and $+f_o$. When this value for $P_x(f)$ is substituted into Equation (27) the result for the truncated P'(f) is

$$P'_x(f) = \frac{A^2}{2} \frac{\sin[2\pi T(f-f_o)]}{2\pi(f-f_o)} + \frac{A^2}{2} \frac{\sin[2\pi T(f+f_o)]}{2\pi(f+f_o)} \qquad [30]$$

For positive frequencies where

$$0 \ll \frac{1}{T} \ll f_o,$$

$$P'_x(f) = \frac{A^2}{2} \frac{\sin[2\pi T(f-f_o)]}{2\pi(f-f_o)} \qquad [31]$$

The maximum $P'_x(f)$ is reached when the denominator approaches zero ($f \to f_o$). Since an indeterminant form is reached (0/0) when the limit is applied, the maximum $P'_x(f)$ is determined by L'Hospital's rule to be

$$P'_x(f) = \lim_{f \to f_o} \left[\frac{A^2}{2} \frac{\frac{d}{dt}[\sin 2\pi T(f-f_o)]}{\frac{d}{df} 2\pi(f-f_o)} \right] \qquad [32]$$

$$= \lim_{f \to f_o} \frac{A^2}{2} \frac{2\pi T \cos 2\pi T(f-f_o)}{2\pi} = \frac{A^2 T}{2} \qquad [33]$$

As T gets larger, the peak becomes higher and narrower, until T approaches infinity, when $P'_x(f)$ approaches a delta function. Since T is finite, what would have been a very sharp peak with the power concentrated within a very narrow frequency range now has become a shorter, broader curve with the power spread out due to the (sin x)/x term as shown in Figure (A1). This spread of power is termed leakage.

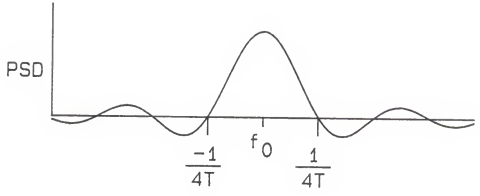

Figure A1. Boxcar function window

The first zero crossing to the right will occur at 1/4 of the cycle.

$$2\pi T(f_r - f_o) = \frac{\pi}{2}$$

$$f_r = f_o + \frac{1}{4T}$$

For the left side, the first zero crossing occurs at $f_l = f_o - \frac{1}{4T}$. The spread of the curve is thus due only to the length of data sample:

$$f_r - f_l = f_o + \frac{1}{4T} - \left[f_o - \frac{1}{4T}\right] = \frac{1}{2T} \qquad [34]$$

The areas to the side of the main peak, referred to as side lobes, may be of a significant size and cause the main peaks to be distorted, particularly if frequencies in the data are located close together and the side lobes happen to be in phase so that they are additive. The distinct beginning and end of the data have the effect of inserting a (sin x)/x term. The spreading cannot be eliminated, but different windows, as the the type of function (sin x)/x is referred to, may be used to increase the height of the main peak or increase the spread of the main peak. These windows can operate directly on the data in time domain or on the transformed values in the frequency domain. A data window operates in the time domain for a given interval with the effect of multiplying data or signals that are defined for a longer period and which will then be subjected to further processing.

Windows may seem to be a complicating addition, but they are unavoidable. By default, the window present is the basic boxcar, which has some undesirable characteristics that can be reduced by other windows. These windows tend to smooth the data for improved quality in the frequency analysis. The categories of lag and spectral windows appear most often in literature. The lag windows are a function of lag, a time difference between two events considered together. These windows exist for a certain interval and then vanish. Their counterparts in the frequency domain are the spectral windows. Blackman and Tukey (1958,pp.95-99) list five possible lag-spectral window pairs. The boxcar window, inherent in finite data was discussed above. Two windows that were considered in the data analysis were the hanning and hamming window.

The hanning window is defined by

$$= 0 \qquad \tau < -T_m$$

$$u_{T_m}(\tau) = \frac{1}{2}\left(1 + \cos\frac{\pi\tau}{T_m}\right) \qquad -T_m \leq \tau \leq T_m \qquad [35]$$

$$= 0 \qquad \tau > T_m$$

T_m is the length of autocorrelation used.
The Fourier transform of this is

$$U_{T_m}(f) = \frac{1}{2}U_{T_m}(f) + \frac{T_m}{2}\left[\frac{\sin\left[T_m(2\pi f - \frac{\pi}{T_m})\right]}{T_m(2\pi f - \frac{\pi}{T_m})} + \frac{\sin[T_m(2\pi f + \frac{\pi}{T_m})]}{T_m(2\pi f + \frac{\pi}{T_m})}\right] \qquad [36]$$

$$= \frac{1}{2}U_{T_m}(f) + \frac{1}{4}U_{T_m}(f - \frac{1}{2T_m}) + \frac{1}{4}U_{T_m}(f + \frac{1}{2T_m}). \qquad [37]$$

Thus the hanning window turns out to be the summation of three of the boxcar functions. Since these lobes are spaced $1/(2T_m)$ Hz apart, the hanning window has the effect of averaging three adjacent lobes and giving the center one twice as much weight as the end pair, reducing the center lobe to 1/2 of its

former height, but also doubling its width. The distance between the first zero crossings on either side of the main lobe is now $2/T_m$ while the effective bandwidth, the frequency interval between half power points, is now $1/T_m$.

The second spectral window is the hamming window, defined by

$$= 0 \qquad \tau < -T_m$$

$$u_{T_m}(\tau) = .54 + .46 \cos \frac{\pi\tau}{T_m} \qquad -T_m < \tau < T_m \qquad [38]$$

$$= 0 \qquad \tau > T_m$$

After Fourier transform,

$$U_{T_m}(f) = .54\, U_{T_m}(f) + .23\, U_{T_m}\left(f + \frac{1}{2T_m}\right) + .23\, U_{T_m}\left(f - \frac{1}{2T_m}\right) \qquad [39]$$

So, the hamming window is similar to the hanning window in that they are both sums of (sin x)/x terms, but with different weights. Two differences between them can be noted:

1. The height of the maximum side lobe for the hamming window is approximately 1/5 that of the hanning window.

2. The heights of the side lobes of the hanning window drop more rapidly than do those of the hamming window.

Thus one difference favors the hamming and the other favors the hanning window.

For either the hanning or hamming window, the adjacent side lobes with their positive and negative values will tend to cancel. If the spectrum has a strong power level at a distance which is resonant with a low main peak and the negative side lobes tend to cancel it out, the low peak can still be noted by the presence of the side lobes. Confidence intervals for spectral densities can be obtained by using both a positive window such as Parzen's and a negative window (See Wonnacott (1961)).

Discrete Spectra

The popularity of digital data collection indicates that discrete intervals may be of more use. Accordingly, the equations are modified to handle discrete data by using summations rather than integrals and Δt instead of dt. The following approach, which has been described by Blackman and Tukey (1958) and Otnes and Enochson (1972 p.270), has been used to compute the power spectral density (Walls, et al., 1954) and (Wendenborn, 1966).

1. Let X be a sequence of N evenly-spaced points having a zero mean; if this is not the case, find the mean and use the set of standard deviations. Wendenborn (1966) and Walls, et al. (1954) use a running average to

eliminate the low frequency cycles that would not be adequately represented in the data.

2. The sample autocorrelation R_r is calculated for (m+1) values where m represents the maximum "time" lag. Since the data is evenly spaced, the total time represented is $m\Delta t$, so the number lag becomes a time lag.

$$R_r = \frac{1}{N-r} \sum_{i=1}^{N-r} x_i x_{i+r} \qquad r = 0,1,\ldots m \qquad [40]$$

3. The power spectral density is calculated for various frequencies, using trapezoidal integration.

$$P'_r(f) = \frac{\Delta t}{\pi}\left[R_o + 2 \sum_{q=1}^{m-1} R_q \cos \frac{\pi r q}{m} + R_m \cos \pi r\right] \qquad [41]$$

These $P'_r(f)$ values are at evenly-spaced frequencies (rad/unit time) given by

$$f = \frac{r\pi}{m\,\Delta t} \qquad r = 0,1,\ldots,m \qquad [42]$$

4. These raw spectral density estimates are then smoothed using a spectral window. For example, if the hamming window is used:

$$P_r''(f) = .23\ P'_{(q-1)}(f) + .54\ P'(f)_q + .23\ P'_{(q+1)}(f) \qquad q \neq 0,m \qquad [43]$$

$$P''_0(f) = .54\ P'_0(f) + .46\ P'_1(f) \qquad [44]$$

$$P''_m(f) = .46\ P'_{m-1}(f) + .54\ P'_m(f) \qquad [45]$$

Step 3 could be done by alternate methods, such as the Fast Fourier Transform, that would decrease the computer time needed if the data is evenly spaced. For equally-spaced data, the frequency range of the estimated spectrum ranges from 0 to $1/(2\Delta t)$, the Nyquist folding frequency. Any frequency present in the data that is higher than the folding frequency will be represented, by aliasing, in the principal part of the spectrum. When $0 < f < 1/2\Delta t$, f is called the principal alias and could possibly represent its aliases f, $2f_N$-f, $2f_N$+f, $4f_N$-f, $4f_N$+f, etc., with f_N equal to the Nyquist frequency.

The discrete method was the first attempt to analyze the data. Individual minutes of fine data were analyzed and the resulting spectra were averaged to obtain an "overall" spectra. Sequences of coarse data (minute averages) were also analyzed for low frequency patterns. The results from the second analysis were not practical for a regenerated data cycle of 10-15 minutes and the results from analyzing just 15 points at a time were inconclusive so a longer series was proposed by recombining the data. The literature listed no method to recombine data with unusual spacing so Blackman-Tukey's approach for evenly-spaced discrete data was abandoned.

APPENDIX B - DIRECT QUADRATIC SPECTRUM ESTIMATION

Ways of handling a real data sample for the discrete evenly-spaced case have been discussed in Appendix A. Further work on time series has generated methods of dealing with gaps in data and even irregularly-spaced data. One method for dealing with irregular-spaced data is the Direct Quadratic Spectrum Estimation (DQSE) method developed by Marquardt and Acuff. This appendix summarizes the DQSE method (Marquardt and Acuff, 1984) which was used to determine the spectrum for the data on an irregular-space basis.

Several assumptions are necessary to apply the DQSE method. It is assumed that the pattern of irregular spacing is not related to the stochastic properties of the process y(t) being sampled, where the independent variable t represents either time or distance units. The process y(t) is assumed to be at least weakly stationary, meaning that the covariance between two points t_i and t_j, where $t_i < t_j$, depends only on the time difference $(t_j - t_i)$. The mean is assumed to be zero. The data comes from a process y(t) in which observations are made at times t_i during a single, continuous period of observation [0,T]. Data is in the form (t_i, Y_i), where i=1,2,3,...n and $0 \leq t_i \leq T$.

The maximum frequency range of the spectrum, if evenly spaced, is from 0 to $1/(2\Delta t)$; any frequency in the data which is higher than the folding frequency is represented by its alias. For irregularly spaced data, the cutoff point for folding is less sharp, particularly so as the spacing becomes more random. The sensitivity to high frequency cycles below the Nyquist frequency is diminished, but some cycles above the cutoff frequency can be obtained. Jones (1962) provides a theoretical base for the direct quadratic spectrum estimation using irregular data.

The DQSE equation takes the form

$$P(\omega) = \frac{1}{T'} \sum_{i<j}^{n\ n} W_{ij} Y(t_i) Y(t_j) \qquad [1]$$

T' is the effective record length. Depending on the data spacing, it is equal to the record length or less (see equation (8)).

W_{ij} is the weight represented by the i,j element in the symmetric quadratic form ($W_{ij} = W_{ji}$)

The weight element is dependent on several factors:

$$W_{ij} = D(\tau) F(t_i, t_j) \cos 2\pi\omega \cdot \tau \qquad [2]$$

$D(\tau)$ is the lag window for lag τ, $\tau = t_j - t_i$

$F(t_i, t_j)$ is the "data spacing factor", more precisely defined by equation (9 or 10)

ω frequency in cycles per unit time or distance

The window could be one of those of discussed in Appendix A or another suitable window; the hanning window was used by Marquardt and Acuff. The hamming window gave similar results in the present analysis. So the window takes the form

$$D(\tau) = \frac{1}{2}\left[1 + \cos \pi \frac{\tau}{\tau_m}\right] \qquad \tau \leq \tau_m \qquad [3]$$

$$= 0 \qquad \tau > \tau_m \qquad [4]$$

τ_m is the maximum time (or distance) lag used

The data spacing factor is based on the idea that the weight given to each ij element should be proportional to the time represented by that element. The spacing factor was suggested in work done by Jones (1962). In terms of each i,j element, the data spacing factor is

$$F(t_i, t_j) = \left[\frac{t_{i+1}+t_i}{2} - \frac{t_i+t_{i-1}}{2}\right]\left[\frac{t_{j+1}+t_j}{2} - \frac{t_j+t_{j-1}}{2}\right] \qquad [5]$$

$$= [t_{i(+)} - t_{i(-)}][t_{j(+)} - t_{j(-)}]$$

$$= \delta_i \delta_j$$

The endpoint conditions are $t_{i-1} \geq 0$ and $t_{j+1} \leq T$. For large time increments, the time intervals may be greater than 1/4 of the cycle length, which is the maximum length used for defining the sinusoid, that corresponds to the frequency. Thus, an upper bound is placed on the weight given to an area by limiting $t_{i(+)}$, $t_{i(-)}$, $t_{j(+)}$, and $t_{j(-)}$ where necessary, where

$$t_{i(+)} = \min\left[\left(\frac{t_{i+1} + t_i}{2}\right), \left(t_i + \frac{1}{4\omega}\right)\right], \qquad [6]$$

$$t_{i(-)} = \max\left[\left(\frac{t_i + t_{i-1}}{2}\right), \left(t_i - \frac{1}{4\omega}\right)\right]$$

The δ_j factor is expressed similarly by substituting j in place of i on the right side of the last two equations. End conditions are defined at t = 0 and t = T by setting $t_0 = -t_1$, and $t_{n+1} = 2T - t_n$. When $\omega = 0$, or is still small, the periods are very large, with the possible result of large data gaps being within the minimum δ, and having an undue influence on the spectrum. The value of ω is thus constrained to be

$$\omega(\text{see equation 6}) = \max[\omega, M\omega_M] \qquad [7]$$

The variable, M, is an arbitrary multiplier (.1 is given as an example) and $\omega_M = (n-1)/2T$ is the Nyquist frequency associated with the average inter-point interval in the given record.

Equation (6) implies a decrease in the effective length of time when the data is irregularly spaced or contains gaps. The effective length of $T'(\omega) \leq T$ is defined:

$$T'(\omega) = \sum_{i=1}^{n} \delta_i \qquad [8]$$

The δ_i are defined in equation (6). If the data is evenly spaced with no gaps, the effective length simplies to the actual length for frequencies less than or equal to the folding frequency. For data with large holes, the effective length gets shorter as the frequency increases.

The data spacing factor can be viewed as the result of a discrete integration over the area where, but not including, $t_i = t_j$ to the boundary $t_j = t_i + \tau_m$. See Figure B1 for the nomenclature. Some area outside the squares wholly in the integration area will be included with this approach. This makes the integration area larger than it actually is, leading to a distorted value for the data spacing factor. Hence the following adjustment is made in the equation (5).

$$F(t_i,t_j) = \delta_i\delta_j - A_{ij} \qquad [9]$$

The A_{ij} represents the area to be subtracted from the rectangular local area. The following diagnostic criteria are needed:

P_2: If $t_{j(+)} \leq t_{i(-)} + \tau_m$, then P_2 is inside the domain of integration; otherwise P_2 is outside.

P_1: If $t_{j(-)} \leq t_{i(-)} + \tau_m$, then P_1 is inside the domain of integration; otherwise both P_1 and P_2 are outside.

P_4: If $t_{i(+)} \leq t_{j(+)} + \tau_m$, then P_4 is inside the domain of integration; otherwise both P_2 and P_4 are outside

P_3: If $t_{j(-)} \leq t_{i(+)} + \tau_m$, then P_3 is inside the domain of integration; otherwise P_1, P_2, P_3, and P_4 are outside.

These criteria define the area cut off the local rectangle by the diagonal line $t_j = t_i + \tau_m$. A point on the boundary is defined to be inside the domain. For convenience the following notation is used:

d_{1i} length cut off the rectangle in the i-direction along the side measured from point P_1

d_{2j} length cut off in the j-direction, measured from point P_2, etc.

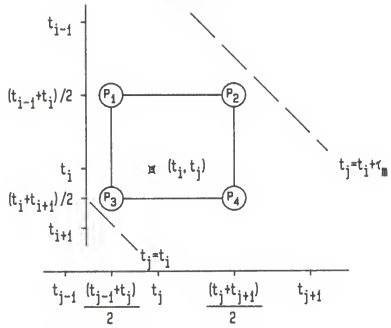

Figure B1a. Nomenclature for a rectangular local area associated with a covariance ordinate.

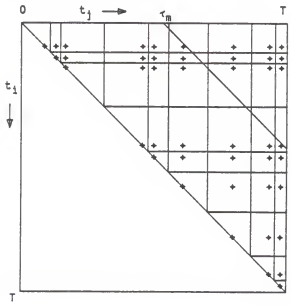

Figure B1b. Example of partial rectangular local areas at domain boundaries.

Source: Marquardt and Acuff (1985, Figure 1a and 1b).

When $t_j - t_i > \tau_m$, the areas of these partial rectangles does not need to be computed since their covariance ordinate location (t_i, t_j) lies outside the

domain of integration, where the lag window $D(\tau)$ is zero. Where the covariance lies inside the domain of integration, the following cases could apply.

Case 1: P_2 is inside

$$A_{ij} = 0$$

Case 2: P_2 is outside. P_1, P_3, and P_4 are inside. Then

$$d_{2j} = t_{j(+)} - t_{i(-)_m} > 0.$$

$$A_{ij} = d_{2j}^2/2.$$

Case 3: P_1 and P_2 are outside. P_3 and P_4 are inside. Then

$$d_{1i} = t_{j(-)} - t_{i(-)} - \tau_m > 0$$

$$d_{2j} = t_{j(+)} - t_{j(-)} > 0$$

$$d_{2i} = t_{j(+)} - t_{i(-)} - \tau_m > 0.$$

$$A_{ij} = (d_{1i} + d_{2i})d_{2j}/2.$$

Case 4: P_2 and P_4 are outside. P_1 and P_3 are inside. Then

$$d_{2i} = t_{i(+)} - t_{i(-)} > 0$$

$$d_{2j} = t_{j(+)} - t_{i(-)} - \tau_m > 0$$

$$d_{4j} = t_{j(+)} - t_{i(+)} - \tau_m > 0$$

$$A_{ij} = (d_{2j} + d_{4j})d_{2i}/2.$$

Case 5: P_1, P_2, and P_4 are outside. P_3 is inside. Then

$$d_{2i} = t_{i(+)} - t_{i(-)} > 0$$

$$d_{2j} = t_{j(+)} - t_{j(-)} > 0$$

$$d_{1i} = t_{j(-)} - t_{i(-)} - \tau_m > 0$$

$$d_{4j} = t_{j(+)} - t_{i(+)} - \tau_m > 0.$$

$$A_{ij} = d_{2i}d_{4j} + (d_{1i}+d_{2i})(d_{2j} - d_{4j})/2.$$

Case 6: If the period of observation begins before the first time point ($t_1 > 0$), or if $t_n < T$, the local areas at the ends of the domain of integration are given by the definitions for the endpoints and bounded by equation (6).

Case 7: The covariance ordinates on the main diagonal where i = j are not used, although some of the area is within the integration area. The triangular region above the main diagonal can be associated with the areas of the "above" and "right" rectangles. The area is split between these two regions by perpendiculars from the main diagonal connecting to the point P_4 of the rectangle above in the integration area and from the main diagonal to the point P_1 of the triangle to the right. When the area is unaffected by the restraints of the minimum time increment for the Nyquist folding frequency, the points P_4 and P_1 coincide. Case 7 applies only to the points on the main diagonal with the associated rectangles for which j = i + 1. The data spacing factor is then modified by adding the area of the triangles.

$$F(t_i,t_j) = \delta_i\delta j - A_{ij} + B_{ij}, \quad \text{when } j=i+1 \qquad [10]$$

There are five possible subcases.

7.1

$$\text{If } t_{i(+)} < \frac{t_{i+1} + t_i}{2} \text{ and/or } t_{j(-)} > \frac{t_j + t_{j-1}}{2}$$

then the point P_3 for the rectangle is constrained away from the main diagonal and $B_{ij} = 0$.

7.2

$$\text{If } t_{i(+)} + (t_{j(+)} - t_{j(-)})/2 < t_i + \frac{1}{4\omega}$$

then the entire triangular area below the rectangle is appended to the rectangle, and $B_{ij} = (t_{j(+)} - t_{j(-)})^2/4$.

7.3

$$\text{If } t_{j(-)} - (t_{i(+)} - t_{i(-)})/2 > t_j - \frac{1}{4\omega}$$

then the entire triangular area to the left of the rectangle is appended to the rectangle, and $B_{ij} = (t_{i(+)} - t_{i(-)})^2/4$.

7.4

$$\text{If } t_{i(+)} < (t_i + \frac{1}{4\omega}) < (t_{i(+)} + (t_{j(+)} - t_{j(-)})/2)$$

then a trapezoidal area below the rectangle is appended and

$$B_{ij} = (t_i + \frac{1}{4\omega} - t_{i(+)})(t_{j(-)} - t_i - \frac{1}{4\omega}). \qquad [11]$$

7.5

$$\text{If } (t_{j(-)} - (t_{i(-)} - t_{i(-)}/2) < (t_j - \frac{1}{4\omega}) < t_{j(-)}$$

then a trapezoidal area to the left of the rectangle is appended and

$$B_{ij} = (t_{j(-)} - t_j + \frac{1}{4\omega})\ (t_j - \frac{1}{4\omega} - t_{i(-)})$$

To follow the recommendation of Marquardt and Acuff, the spectral window is evaluated in parallel with the estimation of the spectrum. The window has the shape

$$Z^*(\omega) = \frac{1}{T'} \sum_{i<j}^{n\ n} W_{ij} = \frac{1}{T'} \sum_{i<j}^{n\ n} D(\tau)\ F(t_i, t_j) \cos 2\pi\omega(\tau). \qquad [12]$$

When working with evenly spaced data, $Z^*(\omega)$ is a periodic function of ω, the sharp center lobe being repeated at all even multiples of the Nyquist frequency. This property leads to 100 percent aliasing of all frequencies above the folding frequency. When dealing with irregularly spaced data, $Z^*(\omega)$ is an almost periodic function, with the possibility of having important side lobes far from the center lobe and within the principal frequency. Due to the nature of irregularly spaced data, the spectral window has two moderate deficiencies when dealing with irregular instead of even data:

1. The center-lobe is less sharp, which leads to somewhat higher variances of the spectral estimates.

2. Care must be taken in interpreting the estimated spectra due to the possibility of partial aliasing if important side lobes are present in the actual window.

The weights in the DQSE quadratic form will change with each set of data due to the change in spacing. They can be adjusted to sharpen the shape to yield a good window. Characteristics of a good window include a sharp center lobe, minimum area outside the center lobe, being positive almost everywhere, by constraint if necessary, and sometimes smoothness. Marquardt and Acuff (1982) show examples of the DQSE method without the B_{ij} factor and discuss both the spectrum and the window.

APPENDIX C

ACTUAL AND REGENERATED DATA

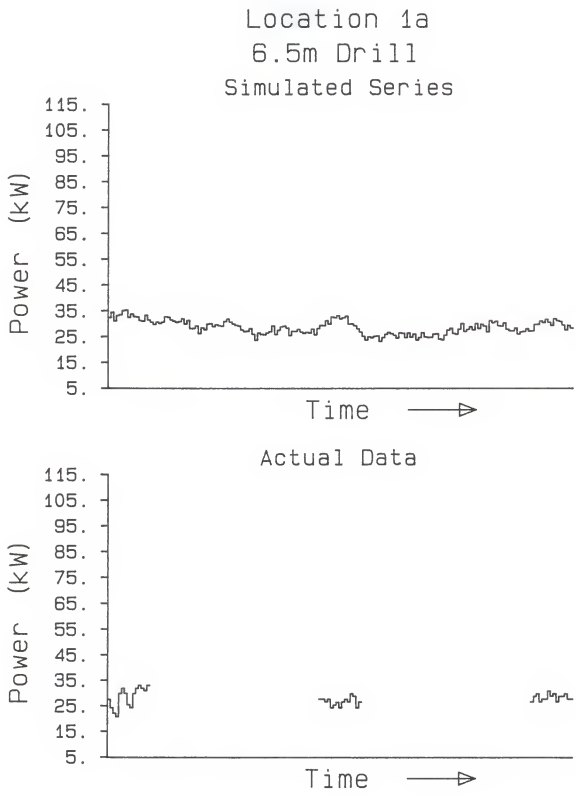
Location 1a
6.5m Drill
Simulated Series
Power (kW)
115.
105.
95.
85.
75.
65.
55.
45.
35.
25.
15.
5.
Time
Actual Data
Power (kW)
115.
105.
95.
85.
75.
65.
55.
45.
35.
25.
15.
5.
Time

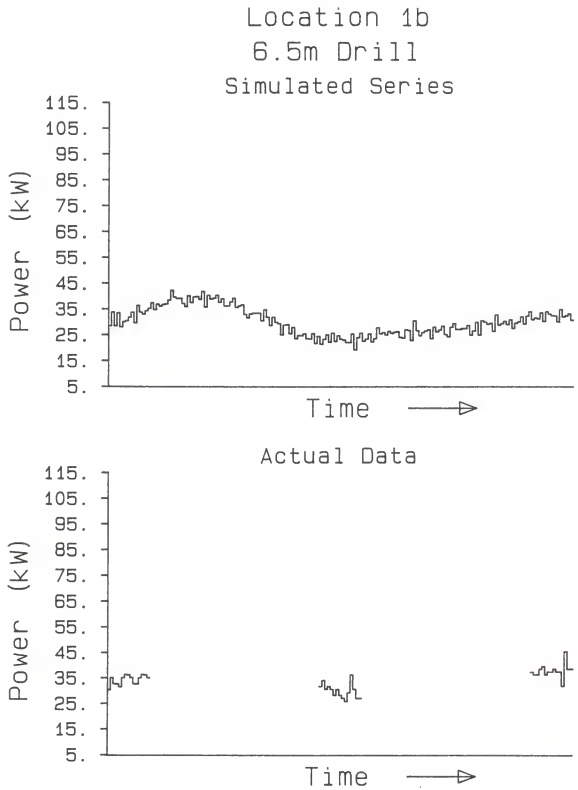
Location 1b
6.5m Drill
Simulated Series
Power (kW)
115.
105.
95.
85.
75.
65.
55.
45.
35.
25.
15.
5.
Time
Actual Data
Power (kW)
115.
105.
95.
85.
75.
65.
55.
45.
35.
25.
15.
5.
Time

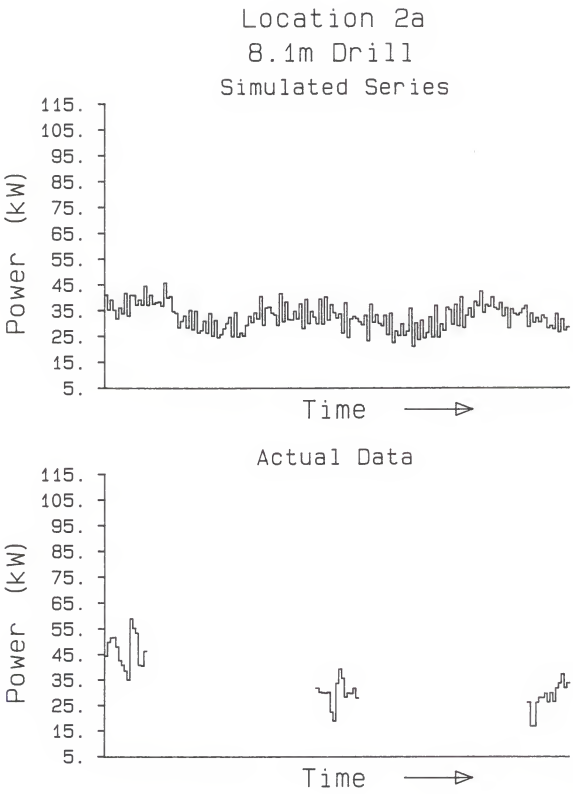
Location 2a
8.1m Drill
Simulated Series
Power (kW)
115.
105.
95.
85.
75.
65.
55.
45.
35.
25.
15.
5.
Time
Actual Data
Power (kW)
115.
105.
95.
85.
75.
65.
55.
45.
35.
25.
15.
5.
Time

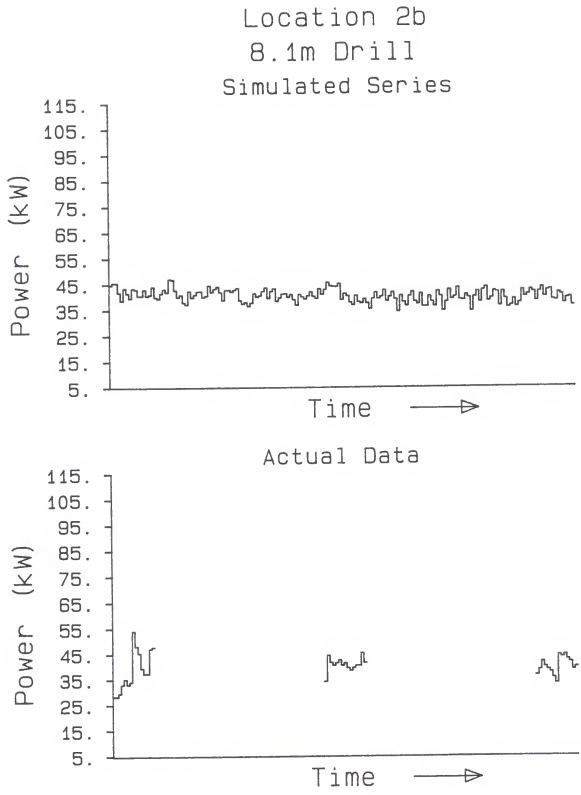
Location 2b
8.1m Drill
Simulated Series
Power (kW)
115.
105.
95.
85.
75.
65.
55.
45.
35.
25.
15.
5.
Time
Actual Data
Power (kW)
115.
105.
95.
85.
75.
65.
55.
45.
35.
25.
15.
5.
Time

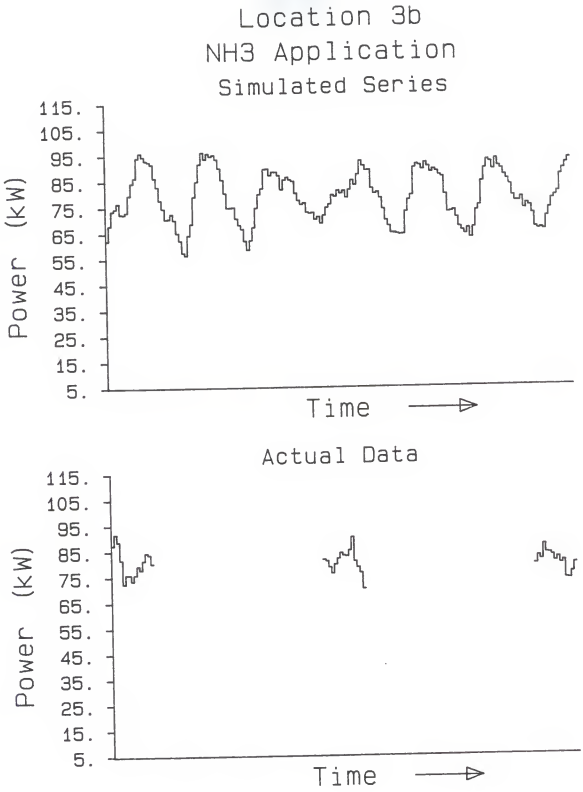
Location 3b
NH3 Application
Simulated Series
Power (kW)
115.
105.
95.
85.
75.
65.
55.
45.
35.
25.
15.
5.
Time
Actual Data
Power (kW)
115.
105.
95.
85.
75.
65.
55.
45.
35.
25.
15.
5.
Time

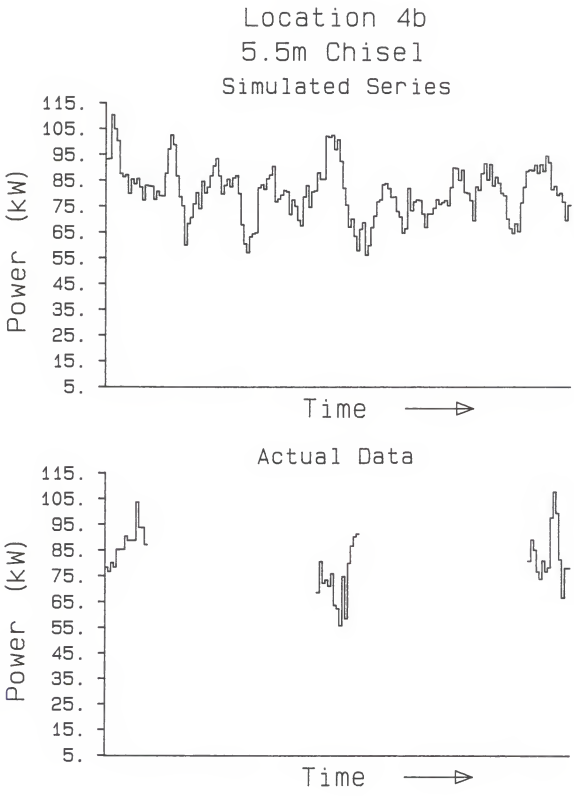
Location 4b
5.5m Chisel
Simulated Series
Power (kW)
115.
105.
95.
85.
75.
65.
55.
45.
35.
25.
15.
5.
Time
Actual Data
Power (kW)
115.
105.
95.
85.
75.
65.
55.
45.
35.
25.
15.
5.
Time

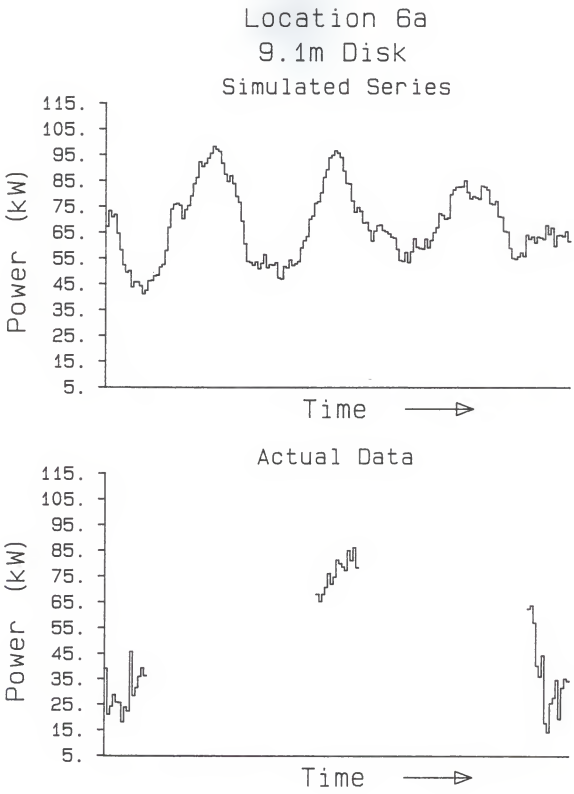
Location 6a
9.1m Disk
Simulated Series
Power (kW)
115.
105.
95.
85.
75.
65.
55.
45.
35.
25.
15.
5.
Time
Actual Data
Power (kW)
115.
105.
95.
85.
75.
65.
55.
45.
35.
25.
15.
5.
Time

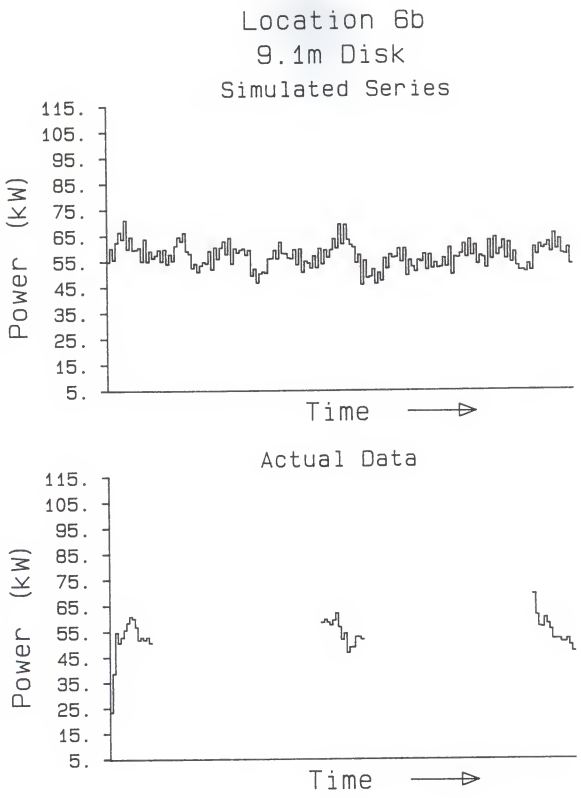
Location 6b
9.1m Disk
Simulated Series
Power (kW)
115.
105.
95.
85.
75.
65.
55.
45.
35.
25.
15.
5.
Time
Actual Data
Power (kW)
115.
105.
95.
85.
75.
65.
55.
45.
35.
25.
15.
5.
Time

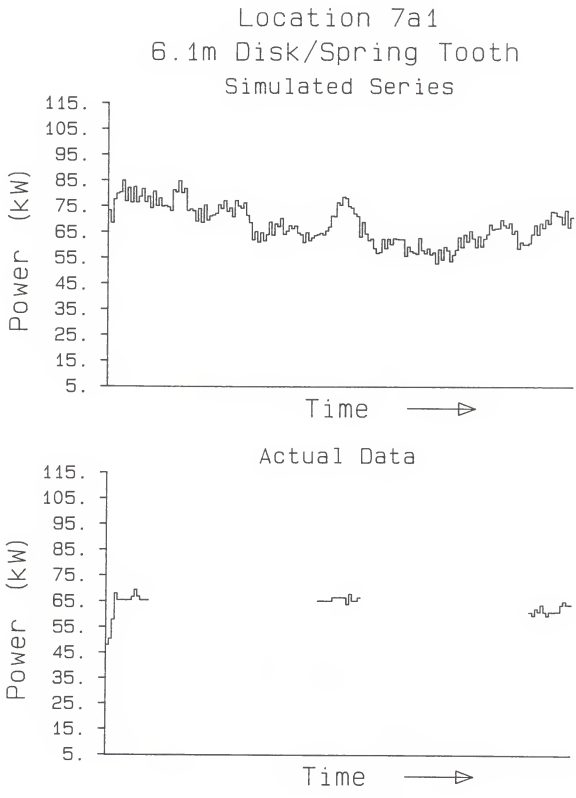
Location 7a1
6.1m Disk/Spring Tooth
Simulated Series
Power (kW)
115.
105.
95.
85.
75.
65.
55.
45.
35.
25.
15.
5.
Time
Actual Data
Power (kW)
115.
105.
95.
85.
75.
65.
55.
45.
35.
25.
15.
5.
Time

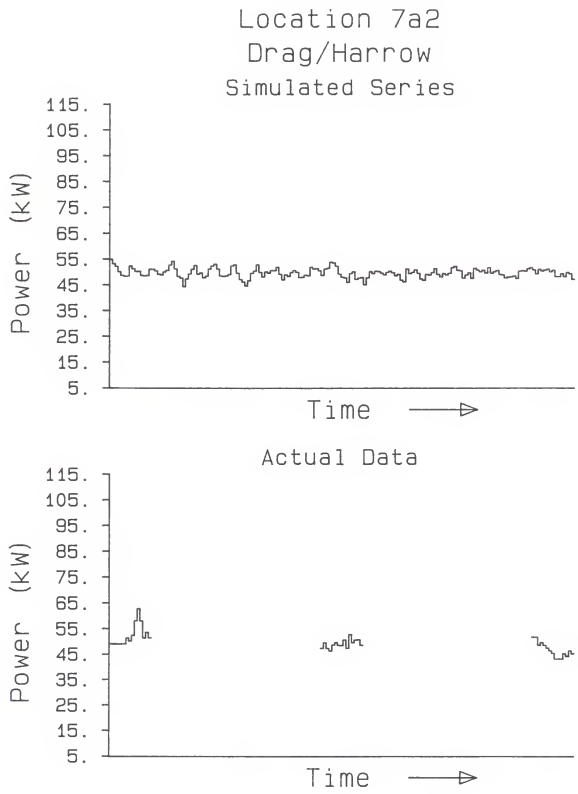
Location 7a2
Drag/Harrow
Simulated Series
Power (kW)
115.
105.
95.
85.
75.
65.
55.
45.
35.
25.
15.
5.
Time
Actual Data
Power (kW)
115.
105.
95.
85.
75.
65.
55.
45.
35.
25.
15.
5.
Time

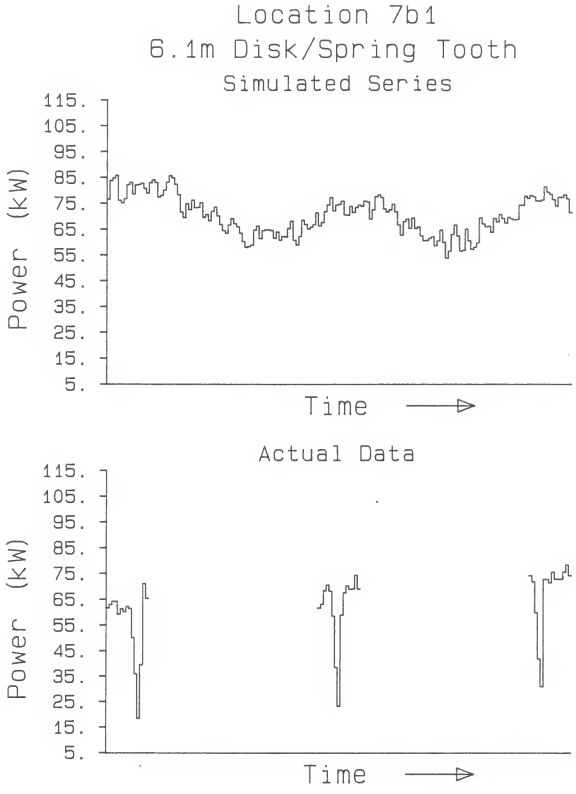
Location 7b1
6.1m Disk/Spring Tooth
Simulated Series
Power (kW)
115.
105.
95.
85.
75.
65.
55.
45.
35.
25.
15.
5.
Time
Actual Data
Power (kW)
115.
105.
95.
85.
75.
65.
55.
45.
35.
25.
15.
5.
Time

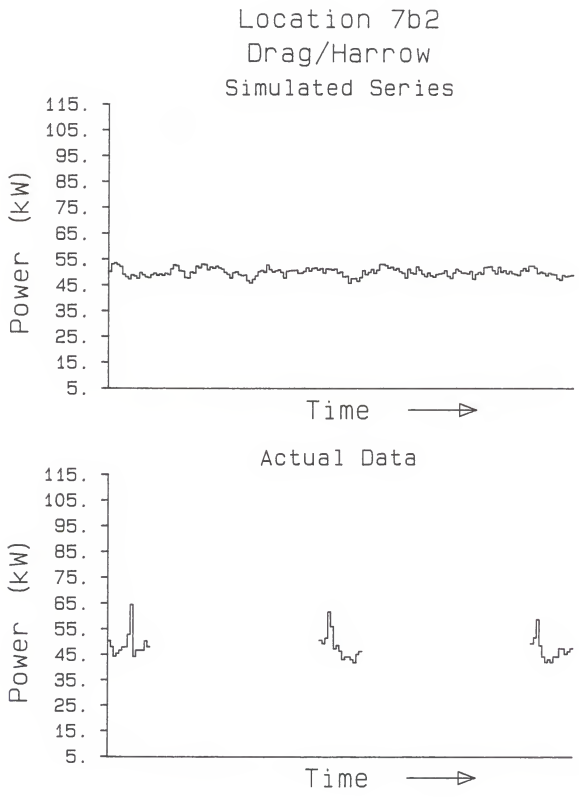
Location 7b2
Drag/Harrow
Simulated Series
Power (kW)
115.
105.
95.
85.
75.
65.
55.
45.
35.
25.
15.
5.
Time
Actual Data
Power (kW)
115.
105.
95.
85.
75.
65.
55.
45.
35.
25.
15.
5.
Time

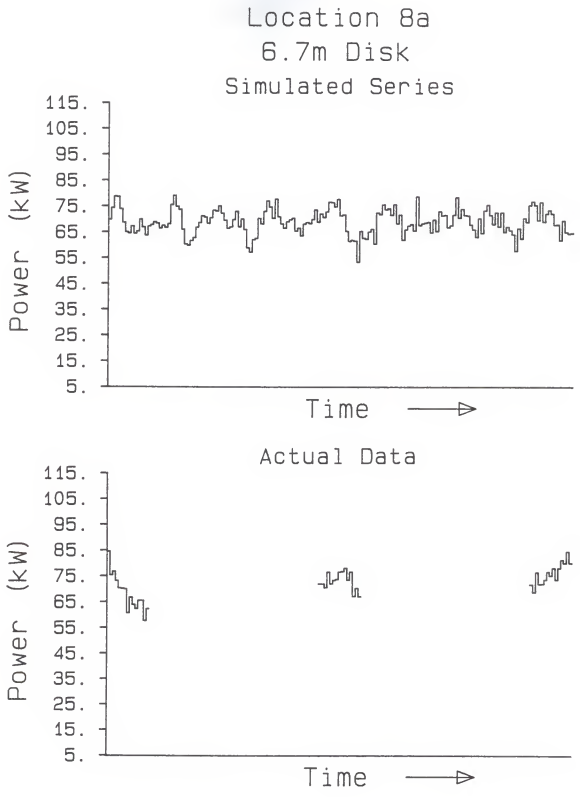
Location 8a
6.7m Disk
Simulated Series
Power (kW)
115.
105.
95.
85.
75.
65.
55.
45.
35.
25.
15.
5.
Time
Actual Data
Power (kW)
115.
105.
95.
85.
75.
65.
55.
45.
35.
25.
15.
5.
Time

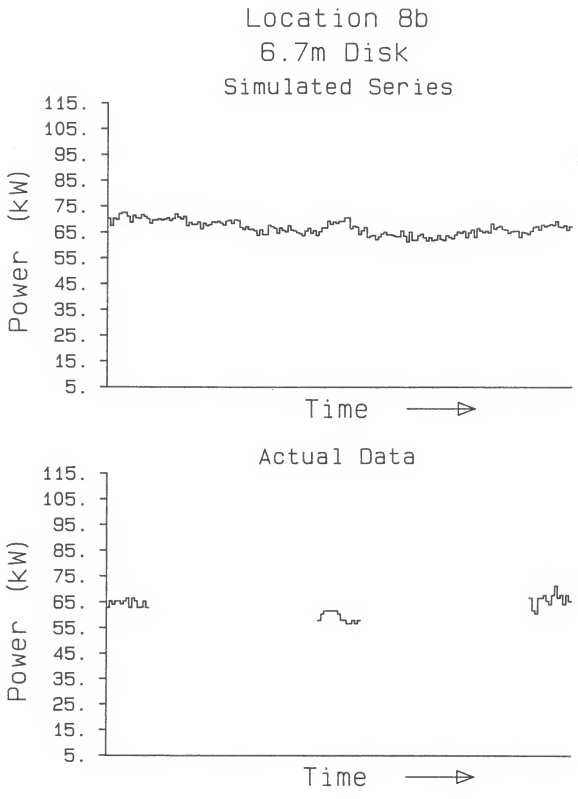
Location 8b
6.7m Disk
Simulated Series
Power (kW)
115.
105.
95.
85.
75.
65.
55.
45.
35.
25.
15.
5.
Time
Actual Data
Power (kW)
115.
105.
95.
85.
75.
65.
55.
45.
35.
25.
15.
5.
Time

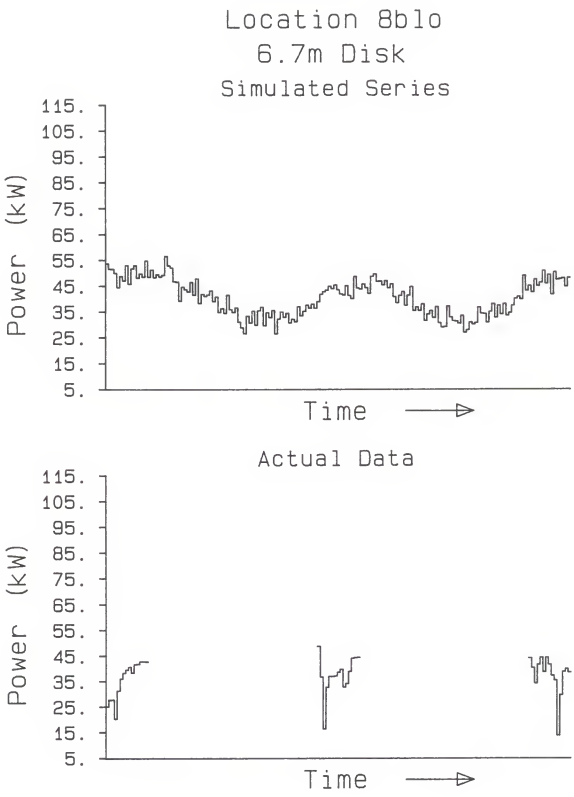
Location 8b1o
6.7m Disk
Simulated Series
Power (kW)
115.
105.
95.
85.
75.
65.
55.
45.
35.
25.
15.
5.
Time
Actual Data
Power (kW)
115.
105.
95.
85.
75.
65.
55.
45.
35.
25.
15.
5.
Time

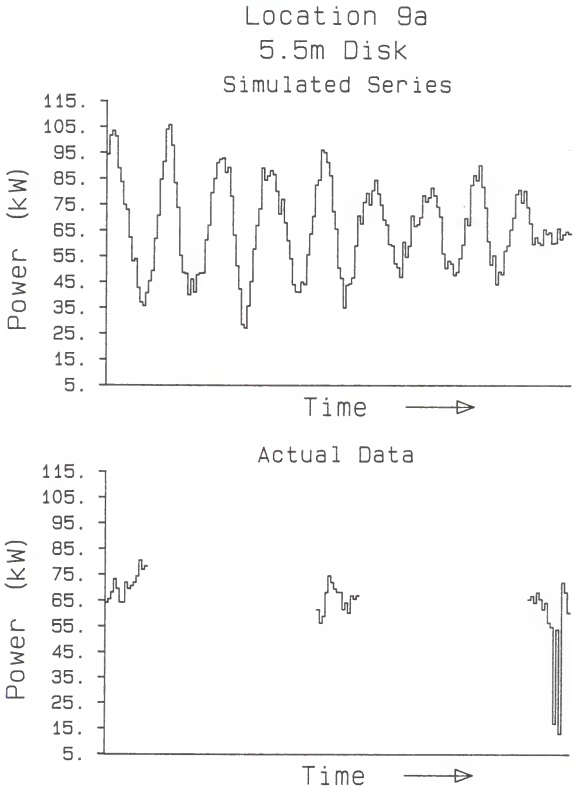
Location 9a
5.5m Disk
Simulated Series
Power (kW)
115.
105.
95.
85.
75.
65.
55.
45.
35.
25.
15.
5.
Time
Actual Data
Power (kW)
115.
105.
95.
85.
75.
65.
55.
45.
35.
25.
15.
5.
Time

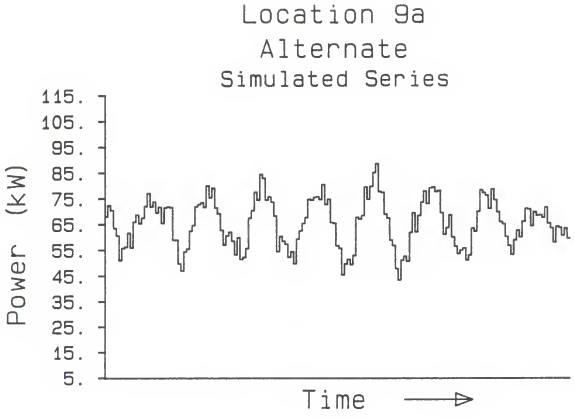
Location 9a
Alternate
Simulated Series
115.
105.
95.
85.
75.
65.
55.
45.
35.
25.
15.
5.
Power (kW)
Time

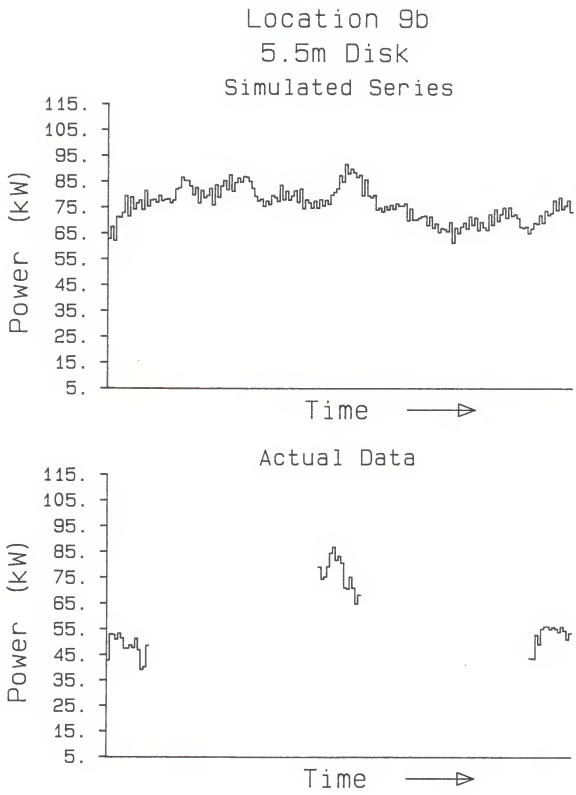
Location 9b
5.5m Disk
Simulated Series
Power (kW)
115.
105.
95.
85.
75.
65.
55.
45.
35.
25.
15.
5.
Time
Actual Data
Power (kW)
115.
105.
95.
85.
75.
65.
55.
45.
35.
25.
15.
5.
Time

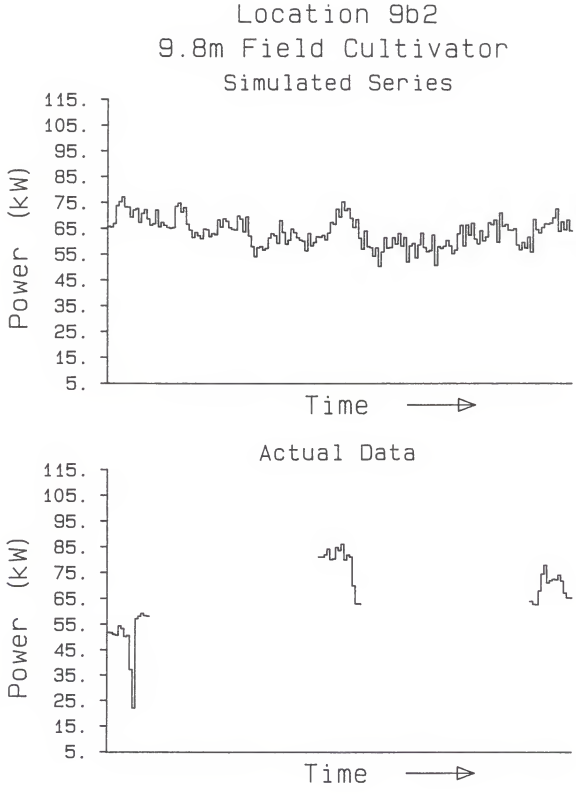
Location 9b2
9.8m Field Cultivator
Simulated Series
Power (kW)
115.
105.
95.
85.
75.
65.
55.
45.
35.
25.
15.
5.
Time
Actual Data
Power (kW)
115.
105.
95.
85.
75.
65.
55.
45.
35.
25.
15.
5.
Time

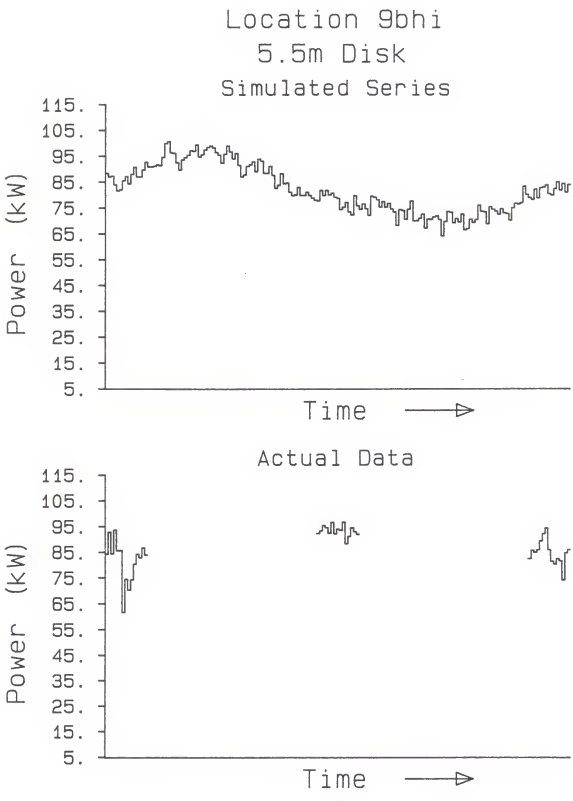
Location 9bhi
5.5m Disk
Simulated Series
Power (kW)
115.
105.
95.
85.
75.
65.
55.
45.
35.
25.
15.
5.
Time
Actual Data
Power (kW)
115.
105.
95.
85.
75.
65.
55.
45.
35.
25.
15.
5.
Time

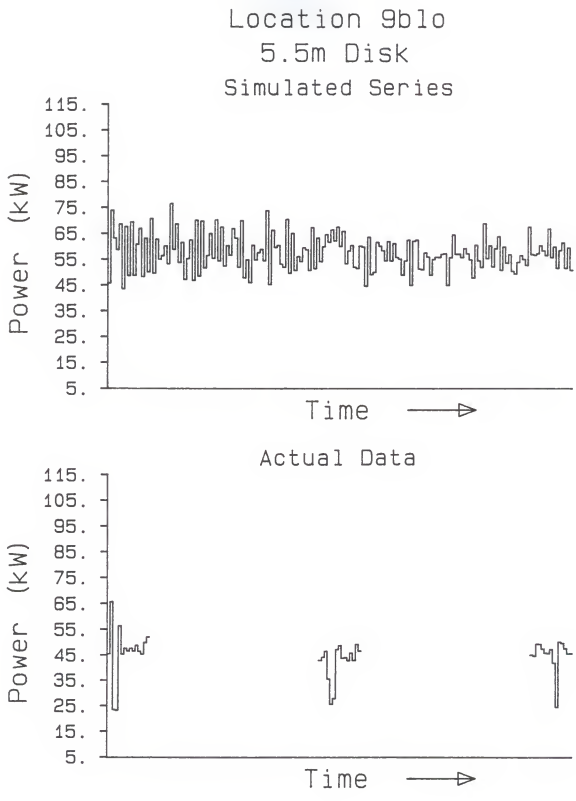
Location 9blo
5.5m Disk
Simulated Series
Power (kW)
115.
105.
95.
85.
75.
65.
55.
45.
35.
25.
15.
5.
Time
Actual Data
Power (kW)
115.
105.
95.
85.
75.
65.
55.
45.
35.
25.
15.
5.
Time

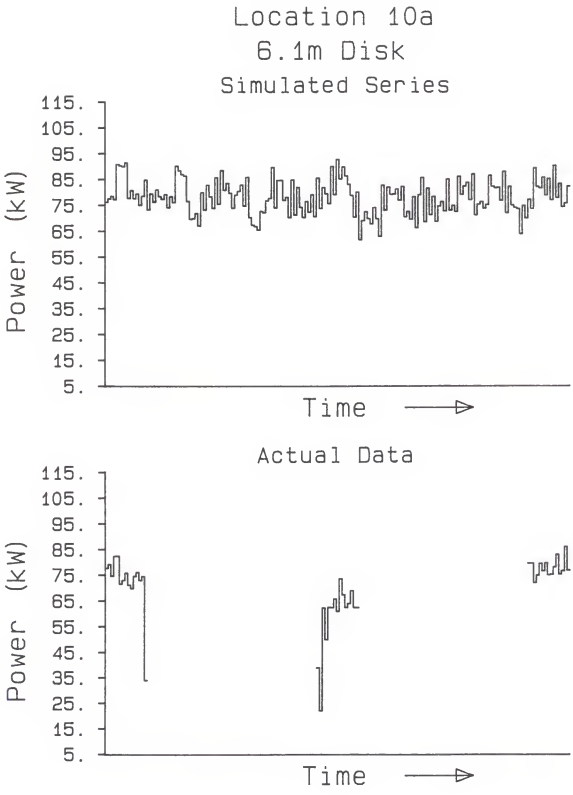
Location 10a
6.1m Disk
Simulated Series
Power (kW)
115.
105.
95.
85.
75.
65.
55.
45.
35.
25.
15.
5.
Time
Actual Data
Power (kW)
115.
105.
95.
85.
75.
65.
55.
45.
35.
25.
15.
5.
Time

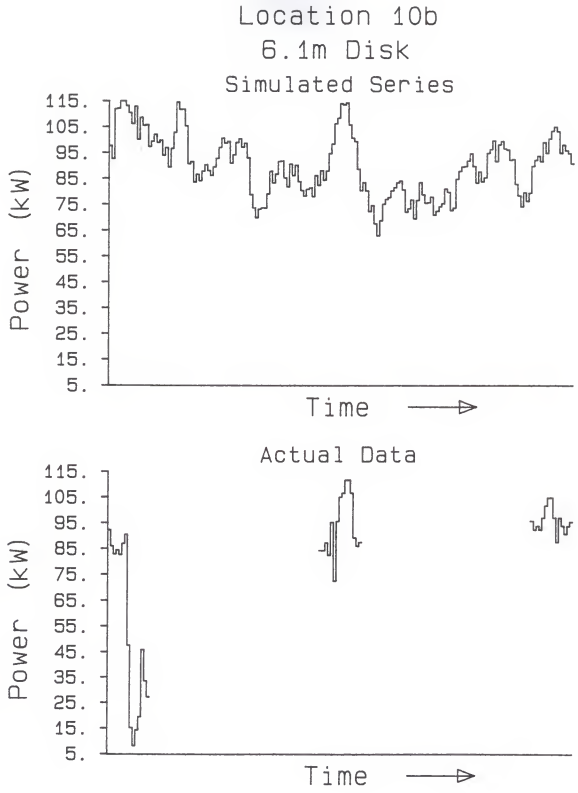
Location 10b
6.1m Disk
Simulated Series
Power (kW)
115.
105.
95.
85.
75.
65.
55.
45.
35.
25.
15.
5.
Time
Actual Data
Power (kW)
115.
105.
95.
85.
75.
65.
55.
45.
35.
25.
15.
5.
Time

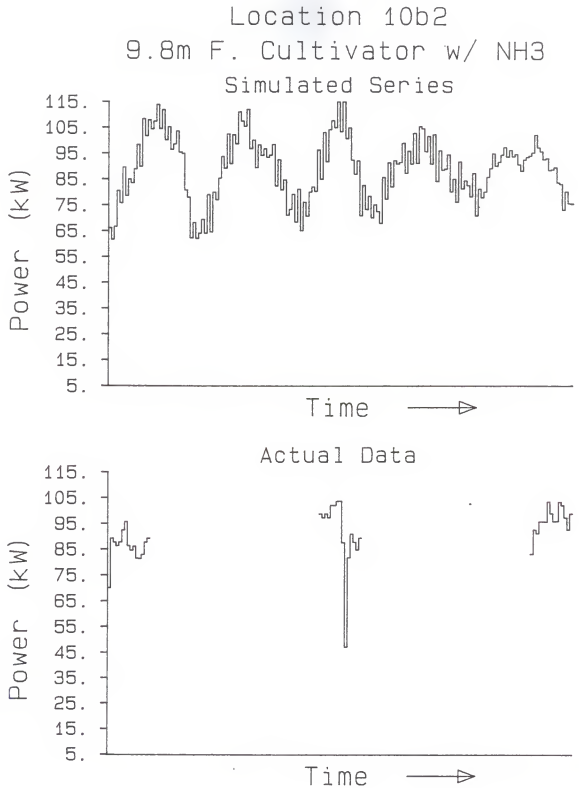
Location 10b2
9.8m F. Cultivator w/ NH3
Simulated Series
Power (kW)
115.
105.
95.
85.
75.
65.
55.
45.
35.
25.
15.
5.
Time
Actual Data
Power (kW)
115.
105.
95.
85.
75.
65.
55.
45.
35.
25.
15.
5.
Time

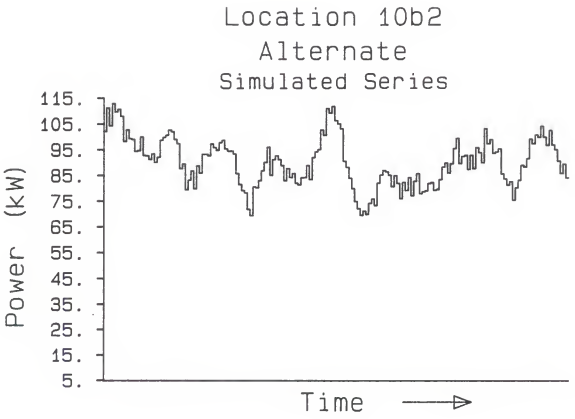
Location 10b2
Alternate
Simulated Series
115.
105.
95.
85.
75.
65.
55.
45.
35.
25.
15.
5.
Power (kW)
Time

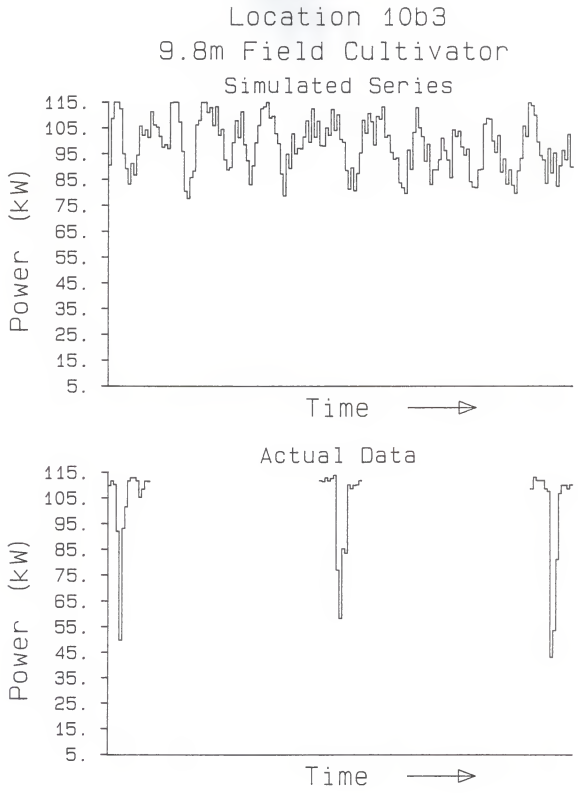
Location 10b3
9.8m Field Cultivator
Simulated Series
Power (kW)
115.
105.
95.
85.
75.
65.
55.
45.
35.
25.
15.
5.
Time
Actual Data
Power (kW)
115.
105.
95.
85.
75.
65.
55.
45.
35.
25.
15.
5.
Time

APPENDIX D

FORTRAN PROGRAM TO REGENERATE TIME SERIES

```
CCCCCCCCCCCCCCCCCCCCCCCCCCCC
C
C     THIS PROGRAM, DARMA.F, GENERATES AN ARMA(6,5) PROCESS USING
C     PARAMETERS COMPUTED BY THE MINIMIZATION OF THE -2 LN(LIKELIHOOD)
C     FUNCTION OR ANY OTHER TEST NUMBERS
C
C     AUTHOR - NAOMI REGIER
C              AGRICULTURAL ENGINEERING
C              SEATON HALL
C              KANSAS STATE UNIVERSITY
C              MS CLASS OF 1986
C
C     IMPORTANT NOTE:  THE ROUTINES, "RANNP" AND "RANN" ARE FROM
C     HARRIS FORTRAN AND MAY NOT BE AVAILABLE ON ALL SYSTEMS.
C
C     THE SUBROUTINE RANNP INITIALIZES THE ARRAY FOR RANN.
C     ITS ARGUMENT IS THE SEED, BY DEFAULT = 1.
C
C     THE FUNCTION RANN IS A REAL RANDOM NUMBER DISTRIBUTED ABOUT
C     A NORMAL DISTRIBUTION CURVE.  ITS FIRST ARGUMENT IS THE MIDPOINT
C     OF THAT CURVE AND THE SECOND ARGUMENT IS THE STANDARD DEVIATION.
C
C     Input is UNIT 7
C     Output is UNIT 8
C
C     VARIABLE LIST
C        INPUT VARIABLES:
C           RMEAN - Desired mean of the regenerated numbers
C           DEV - Standard deviation of the random error input
C           NP - Number of autoregressive parameters
C           NQ - Number of moving average parameters
C           A - Coefficients for autoregressive numbers
C           B - Coefficients for moving average numbers
C        OUTPUT VARIABLES:
C           A, B - Provide label of coefficients at top of file
C           XM - Predicted number with a nonzero mean
C        INTERNAL VARIABLES:
C           COEF - Array of random values, normally distributed,
C                  at time t-1 to t-q
C           X - Array of past predicted values back to time p
C           RNEW - Random value at time t
C           XSUM - Amount due to autoregressive contribution
C           CSUM - Amount due to moving average contribution
C           XNEW - Curent predicted value
C
CCCCCCCCCCCCCCCCCCCCCCCCCCCC
C
      REAL X(6),A(6),B(5),COEF(5)
C Initialize gaussian random number generator
      CALL RANNP(3.)
```

```
C Read input
      READ(7,*) RMEAN
      READ(7,*) DEV
      READ(7,*) NP, NQ
C Read in autoregressive coefficients
      DO 5 I=1,NP
    5 READ(7,*) A(I)
C Read in moving average coefficients
      DO 10 J = 1,NQ
   10 READ(7,*) B(J)
C Write out coefficients
      WRITE(8,2000) A,B
 2000 FORMAT(' ','A: ',6(F6.3,1X),' B: ',5(F6.3,1X))
C Get random numbers for moving average noises
      DO 15 I = 1,NQ
         COEF(I) = RANN(0.,DEV)
   15 CONTINUE
C Initialize X values with zeroes
      DO 20 J = 1,NP
         X(J) = 0.0
   20 CONTINUE
C Recursively generate series of numbers from ARMA(p,q) model
      DO 100 I = NP+1, 600
         RNEW = RANN(0.,DEV)
C Add up autoregressive contribution to present value
         XSUM = 0.
         DO 25 K = 1,NP
   25    XSUM = XSUM + A(K) * X(K)
C Add up moving average contribution to present value
         CSUM = 0.0
         DO 30 KK = 1,NQ
   30    CSUM = CSUM + B(KK) * COEF(KK)
C Present value with zero mean
         XNEW = XSUM + CSUM + RNEW
C Adjust mean to actual
         XM = XNEW + RMEAN
C Reset calculated values for new calculation
         DO 35 J = 0, NP-2
   35    X(NP-J) = X(NP-J-1)
         X(1) = XNEW
C Reset random numbers for next calculation of X
         DO 40 JJ = 0,NQ-2
   40    COEF(NQ-JJ) = COEF(NQ-JJ-1)
         COEF(1) = RNEW
C Discard first 300 values to eliminate effects of initial zeroes
         IF(I .GT. 300) THEN
            WRITE(8,1000) XM
 1000       FORMAT(1X, F10.2)
            ENDIF
  100 CONTINUE
      STOP
      END
```

TIME SERIES ANALYSIS OF POWER REQUIREMENTS FOR TILLAGE TOOLS

by

NAOMI KAY REGIER

B.S., Kansas State University, 1983

AN ABSTRACT OF A MASTER'S THESIS

submitted in partial fulfillment of the

requirements for the degree

MASTER OF SCIENCE

Department of Agricultural Engineering

KANSAS STATE UNIVERSITY
Manhattan, Kansas

1986

ABSTRACT

Evenly-spaced time series with missing values of tractor power loading variations were analyzed by spectral density and autoregressive-moving average (ARMA) methods. The spectral density method was unsatisfactory for easily reproducing a series on the dynamometer and so the coefficients in the ARMA model were found by optimizing the value of -2 ln(likelihood) and selecting the order from among the top five models.

The series for the different tillage tools show some difference between the implements. The drill and drag/harrow have fairly small variations between one point in time and the next. The disk samples generally show a moderately rougher pattern, with variation between the samples. The addition of a springtooth behind the disk did not produce any distinguishable difference. The chisel shows the roughest series while the field cultivator is only slightly smoother. When NH3 is applied, the power increments from one value to the next are small although the general trend may vary.

Appendices include an outline of the basic theory for continuous and discrete evenly, and irregularly-spaced spectral density analysis, as well as graphs of actual data and the series regenerated from the ARMA models. The algorithm for the ARMA model with missing values is given in the main part of the text.